

FINAL REPORT

Determining the Properties and Capabilities of an Existing
Experimental Large Loop EM61 Underwater UXO Detector

SERDP Project MR-1385

December 2006

Peeter Pehme
Dillon Consulting Limited

This document has been cleared for public release



TABLE OF CONTENTS

Executive Summary	v
1.0 Background & Objectives.....	1
2.0 Material and Methods	4
2.1 Dates	4
2.2 Location Details.....	4
2.2.1 Phase I.....	4
2.2.2 Phase II.....	4
2.2.3 Phase III & IV.....	4
2.3 Equipment.....	4
2.4 Targets.....	6
2.5 Deployment.....	6
2.6 Specific Tests.....	8
2.7 Data Processing.....	8
3.0 Results and Accomplishments	11
3.1 Water Conductivity.....	11
3.2 System Variability	12
3.2.1 Rx1 vs Rx2.....	12
3.2.2 Low vs. High Power	13
3.3 Background Variability.....	15
3.4 Geometric Variability	18
3.5 Lateral Response Variation Below the Transmitter.....	20
3.6 Transmitter Size.....	21
3.7 Salinity Variations	22
3.8 Target Responses	24
3.9 Target depth-of-detection.....	24
3.10 Target orientation.....	27
3.11 Response Polarity.....	27
4.0 Conclusions.....	30
4.1 System Noise & Variability.....	30
4.1.1 Receiver Coils.....	30
4.2 Stationary Noise.....	31
4.3 Geometry.....	31
4.4 Response to lateral offsets of Rx and target from the axis of the transmitter.....	31
4.5 Tx Signal Strength	32
4.6 Salinity Variations	32
4.7 Depth Limitations	33
4.8 Response Polarity.....	33
4.9 Modeling.....	34
5.0 Recommendations.....	35

FIGURES

- Figure 1: Schematic Showing Timing (in usec) of Receiver Channels for Geonics EM61 MK2HP
- Figure 2: Various Targets Used for Testing
- Figure 3a: Phase I Testing Set Up
- Figure 3b: Photo of Phase IV Geometry Testing
- Figure 4: EM39 Conductivity Profile Through Water Column
- Figure 5a: R1 & R2, Target A, Rx at 2m, i) Power Mode, ii) High Power Mode
- Figure 5b: F1 & R2, Target B, 1m Below Coils, Rx at 2m & 4m, Low & High Power Modes, Solid Line 1:1 Ratio, Dashed
- Figure 6: Low vs. High Power Decay, R2 at 2m, Target A
- Figure 7: Low vs. High Power Decay, R2 at 1m, Target I
- Figure 8: Background Readings Rx 1 in Low & High Power Modes
- Figure 9a: Correlation of Standard Deviation of Table 7a
- Figure 9b: Correlation of Standard Deviation of Table 7b
- Figure 10a&b: A) Decay Curves for Channel 1, B) Tilted Rx Response with Horizontal Rx Coil Response Subtracted as Rx is Tilt Angles of 6, 11 and 22 Degrees
- Figure 11: Plan View Schematic of Centered and Eight Off-Center Set Ups for Lateral Response Variation Test
- Figure 12a: Lateral Response Variation 1.4 Metres Below Rx
- Figure 12b: Lateral Response Variation 1.4 Metres Below Peak Value
- Figure 13a: Increasing Transmitter Size from 4.3 x 4.3m to 4.3 x 8m has Minimal Effect on Response
- Figure 13b: Schematic Showing the Process of “Folding” Large Loop to a 4.3 x 4.3m Footprint
- Figure 13c: Comparison of Open 4.3 x 8m Loop vs. “Folded” Large Loop to a 4.3 x 4.3 Footprint
- Figure 14a: Fresh vs. Marine Decay Curves for Target A, Low Power Rx 1 at 2 Metres
- Figure 14b: Fresh vs. Marine Decay Curves for Target A, in High Power Mode, Rx 1 at 2 Metres
- Figure 14c: Fresh vs. Marine Decay Curves for Target F
- Figure 15: Depth of 3 Millivolt Threshold for Target A in High Power, Rx 1 in Test I
- Figure 16: Depth of 3 Millivolt Threshold for Target A in Lower Power, Rx 1 in Test IV
- Figure 17: Detection Limits Found by Plotting Signal from Target A 2 Metres Below Receiver Against Receiver Depth
- Figure 18: Detection Limit for Target D Displayed by Plotting Signal from a Target 2 Metres Below Receiver Against Receiver Depth
- Figure 19: Detection Limit for Target I Based on 3 Millivolt Detection Limit
- Figure 20: Comparison of Vertical and Horizontal Decay Curves for Target A Below Receiver
- Figure 21: Target A Lowered .5m Off Side of Rx Coil, Rx at 4m
- Figure 22a: Vertical Cross-Section of Response to Target A
- Figure 22b: Vertical Cross-Section of Response to Target B

TABLES

Table 1:	Fieldwork Dates (all 2005)
Table 2:	Timing of Receiver Channels for Geonics EM61 MK2HP
Table 3:	Description of Various Tests
Table 4:	Example of Correction Applied to Data From One Decay Curve Test for Target C
Table 5:	R2 Response as Percentage of R1
Table 6:	Background Variability, Standard Deviation Values for Figure 8
Table 7a:	Standard Deviation of 60 sec Sampling of the Lower Power Background Data at Various Receiver Depths in Salt Water
Figure 7b:	Standard Deviation of 60 sec Sampling of the High Power Background Data at Various Receiver Depths in Salt Water
Table 9:	Standard Deviation of Lower Power Background Data with Rx1 at 4m and 5m

APPENDICES

Appendix A1 – Geonics’ Time Gate Figure
Appendix A2 – Details of Targets
Appendix A3 – Specific Tests
Appendix A4 – Field Data (Digital)
Appendix A5 – Summary of Tests

LIST OF ACRONYMS

Channel	Also “time gate” a length of time after the turnoff of the transmitter over which the voltage output of the receiver coil is measured (typically a hundred \pm microseconds)
DCL	Dillon Consulting Limited
DND	Department of National Defense (Canadian)
ECC	Environmental Consulting Corporation
HP	High Power mode of transmitter
LP	Low Power mode of transmitter
m	Metre
MS/m	MilliSiemens per metre (unit of electrical conductivity)
Rx1	Receiver Coil 1 (Specially built for DCL, receiver only)
Rx2	Receiver Coil 1 (Standard 1mx.5m underwater receiver/transmitter coil, but only used as receiver)
SERDP	Strategic Environment Research & Development Program
SON	Statement of Need
Tx	Transmitter Coil or Loop
UXO	Unexploded Ordnance

Acknowledgements

Dillon Consulting would like to acknowledge the assistance of our partners Geonics Limited (in particular Miro Bosner) for their / his considerable assistance, discussions and insights. Aeroquest International, specifically Quentin Yarie for his time and creative efforts on our behalf, as well as Steve Balch.

We would like to thank the SERDP program for funding and especially Dr. Anne Andrews for the opportunity to do this work and Anthony Buser for keeping us organized.

Last and, not by any means least, we'd like to thank Dr. John Greenhouse for his considerable scientific and creative inputs as well as providing sound foundations in reality on which we can always rely.

Executive Summary

In response to UXSON-04-03, Dillon Consulting Ltd (DCL) investigated the response of a prototype Large Loop EM61 Marine System. The system was originally conceived in 2002 for a marine UXO survey of Wright's Cove near Halifax, Nova Scotia, to detect accumulations of metal on or below the sea floor at depths of 1 to 15 metres of water. The survey presented new challenges in that the water depths required that sensors be deployed at significant depths, but at the same time contact with the seabed was to be minimized. Dillon Consulting Limited, with assistance from Geonics Limited, modified a high power Geonics EM61-MK2 System by adding a large primary loop transmitter floating on a barge and a submerged receiver mounted on a planing board that was towed beneath the transmitter. The entire system can be purchased for well under \$100K (rented for much less) and does not require a special boat for deployment.

The specific purpose of this research is to determine if the system response of this equipment can be understood and if necessary improved sufficiently to be used for detailed mapping and demonstration phases. The technology targets the near shore environments of critical concern to SERDP, addressing both very shallow (<15 feet, 5 m) and shallow (16-60 feet, 5-20m) water depths. It provides a novel engineering-based technique and platform that overcomes access limitations for locating UXO present in underwater locations. The project also explores the variations of EM response in underwater environments that must be resolved as a necessary precursor to efforts in improving detection and discrimination in underwater UXO-contaminated areas.

The field tests were divided into four phases. The first, third and fourth were undertaken in freshwater and the second in a marine environment. Overall the system performed much as expected although an issue with electrical communication between the receiver and the transmitter proved bothersome. The source of the problem was identified and interim measures taken to minimize the noise.

Adaptations of a mining-based forward modeling program did not prove successful.

The log-log decay curves of field data exhibited excellent fit to linear trends and consistent repeatability indicating a stable response. Background noise, typically less than 3 millivolts on all channels, provides a threshold for the response below which targets can not be detected. For example, with the receiver located 2 m above the bottom, a small projectile (50mm) could be detected in water depths of 4 meters and objects the size of a 55 US gallon drum at 17 metres. Salinity was shown to have influence on the response and detection depth for smaller targets. The response of the system is fairly uniform over a broad area directly below the transmitter leaving the potential for multiple receiver coils. Receiver tilts of less than 20 degrees did not significantly compromise the ability to detect a given target. However misalignment of the receiver does influence the actual values observed which may cause difficulties for discrimination algorithms. Preliminary adaptations to the size and shape of the transmitter were shown to have minimal impact on detection depth.

Future work should concentrate on confirming conclusions regarding the transmitter configurations, on better control of the position and attitude of the receiver relative to the transmitter, and on establishing limitations and noise thresholds for the system when underway. Overall the transmitter-receiver configuration shows promise as an inexpensive detection platform and has potential for adaptation to a variety of systems. It minimizes bottom contact, and has reasonable control of target location and medium water depth capabilities.

1.0 BACKGROUND & OBJECTIVES

In November of 2002 the SERDP program issued a statement of need (SON) for “novel engineering-based technologies or platforms that overcome the access limitations for locating UXO present in underwater locations (e.g. coastal areas, marine sediments, harbors, estuaries, lakes, ponds and wetlands)”. Specifically the SON applied to areas where the water depth was less than 15 feet, designated as “very shallow” or ranged from 15 to more than 60 feet, designated as “shallow”.

The SON also called for projects to develop ways for “improving sensor and signal processing to aid in detection and discrimination in underwater UXO-contaminated areas” and improved understanding of “characterization and phenomenology of underwater UXO, including migration and depth of burial in various underwater environments”.

In January of 2002, Dillon Consulting Limited (DCL), with assistance from Geonics Limited, had modified a high power Geonics EM61-MK2 system to have a large (5x5 metre) floating transmitter loop and a submerged receiver. The goal of that project was to detect accumulations of metal on or below the seafloor at depths of 2 to 60ft (1 to 15 metres) in a cost effective manner and with minimal contact of the seabed. The system was employed at Wright’s Cove, Nova Scotia¹, for Canada’s Department of National Defence (DND). Given time and budget constraints, the system performed well. However, numerous questions regarding the variations and limits of the response arose. Since the system was new, and the approach novel, we could not generally differentiate whether the cause of the variations were a function of this specific technology, a function of EM systems in general, or a phenomena specific to the environment we were working in.

In response to the SON DCL applied to SERDP for research funding to explore both the limitations of the prototype system and (concurrently) the phenomenology of underwater UXO detection with EM systems in general. We were granted a “seed project” (UXO-1835) to initiate the process. Funding was made available in the winter of 2005 and this document reports the results of our efforts.

The first step, and the focus of this seed project, was to acquire a better understanding of the prototype system response and to explore the possibility for modeling that system.

The specific questions relating to system response are:

- What is the “footprint” of the transmitter, that area in the horizontal plane containing the receiver within which the inducing field is effectively constant?
- What is the nature of the system response and how does it vary with geometry and water depth? In particular, under what conditions do the occasional anomaly polarity reversals observed at Wright’s Cove occur?
- How does response vary with water salinity?

¹ 2002, Pehme et al, Adapting the Geonics EM61 for UXO Surveys in 0-20 Meters of Water, Proceedings of the UXO/ Countermine Forum, Orlando, Fl. Session 12.

- What system configuration and transmitter power are required to detect a given target on or beneath the seafloor?
- What are the depth limitations to detecting a given target or accumulation of targets?
- The prototype system components were more or less “off the shelf” with minor tuning. How should they be modified to give optimal performance for a specific range of targets in a given environment?
- What are the main sources of electronic noise in the system and how can they be minimized?

As an alternative to field tests, we were hopeful that some of these questions could be addressed more cost-effectively through the use of numerical models. Our plan was to scale down existing large loop models designed for airborne geophysical applications to the smaller target sizes and depths of interest here. Our intention was to rely on numerical methods if and only if we could establish that the models adequately reproduce responses observed in sea trials.

Unfortunately early attempts at modeling, carried out with the help of personnel at Aeroquest in Milton, Ontario proved unsuccessful due to difficulties in the above-mentioned response scaling. To insure the project maintained it’s focus, numerical modeling was abandoned early in the process and we renewed our emphasis on field-testing.

The field component of this project was initially divided into three main phases:

- I. Ice Test (Fresh Water)
- II. Open Water (Marine)
- III. Open Water (Fresh water)

Phase III was aborted prematurely to deal with technical problems (details below) and a fourth Phase (IV) added to complete the Phase III work.

The primary objectives of Phase I of the fieldwork, carried out on lake ice, were to be:

1. Assemble suitable metallic targets for testing the system response;
2. Test various aspects of the testing methodology, identifying potential areas of improvement;
3. Measure the instrument response to some targets of varying size;
4. Provide data for an initial assessment of numerical modeling capabilities;
5. Test the hypothesis of a geometric basis for the negative values observed in previous work.

Improvements to the test method were implemented as a result of the first phase. It was at this point that the modeling effort proved unsatisfactory and additional emphasize was placed on field-testing.

Phase II, the marine environment test, had as it’s primary objective the gathering of data for the following purposes:

1. Characterization of the noise levels of the system in a variety of configurations;
2. Measuring decay curves for all our targets;
3. Comparison of decay curves using high power (HP) and low power (LP) transmitter settings;
4. Simulation of a misalignment of the RX coil and variation in the geometry of the system;
5. Continued examination of potential causes of polarity inversions in the data.

One of the system issues identified in the Phase II of the project was periodic spikes in the data. These are discussed in detail in the Results section below. The spikes created an inconvenience with respect to assessing the system response to targets and variations in geometry as they relate to differences associated with fresh water and marine environments. Fortunately, the excellent linearity of the response on a log-log plot meant that the low level response could be extrapolated from higher levels with confidence and the extraneous noise did not preclude the usefulness of the data. However, if the system were to be implemented without corrective actions, the spikes would be a critical shortcoming of the system.

The final phase of fresh water testing was intended to fill in gaps in the fresh water data for comparison with the marine data and therefore the tests duplicated many of those conducted in Phase II. At the beginning of Phase III we were able to isolate the source of the extraneous noise spikes to the connection of the receiver coil and demobilized to address the issue. An interim solution was developed and the third Phase was revised into Phase IV with the goals of:

1. Confirming the diagnosis that the source of the spikes was the receiver coil connection;
2. Comparing system responses between a standard receiver coil and the special one built for our system;
3. Completing the Phase I set of target responses in fresh water for comparison with the marine data;
4. Establishing the response variation below the transmitter for comparison with marine data;
5. Examining the variation in response that results from changes in the transmitter loop size.

2.0 MATERIAL AND METHODS

The common details (equipment & targets) of the test phases are described under unified headings. Individual details, unique to the individual phases, are explained as appropriate.

2.1 Dates

The details of the timing of the field work for each phase completed are summarized in Table 1.

Table 1: Field work dates (all 2005):

Phase	Start	End
I	February 28 th	March 1 st
II	July 18 th	July 23 rd
III	October 5 th	October 6 th
IV	October 25 th	October 28 th

Mob/demob not included

2.2 Location Details

2.2.1 Phase I

The field site for the ice test was on Bay's Lake approximately 20 kilometres north of Huntsville, Ontario. The survey set-up was over 16 metres of water, approximately 100 metres off shore. The ice was 0.45 metres thick. The lake bottom is clayey silt of unknown thickness. The bedrock in the area is generally granite and overburden thickness is thin or non-existent.

2.2.2 Phase II

Phase II fieldwork was conducted in Shelburne harbour, approximately 200 kilometres south of Halifax, Nova Scotia. The site was chosen because of its water depth, general low marine activity, adequate distance from fresh water sources, and available logistical support. The water depth varied from 14 metres to over 16 metres depending on the tide. The sea bottom was clay rich and, based on smell, highly organic.

2.2.3 Phase III & IV

The final fresh-water field work was also conducted at Bay's Lake. We moved a short distance from the Phase I test location to an area of the lake where water depths ranged from 20 to 30 metres.

2.3 Equipment

The EM data were collected with a standard Geonics EM61 MK2 instrument and a receiver coil specially adapted for this application. The system console acts as both the transmitter and the receiver control unit. The surface-transmitting coil (Tx) is a multi-turn square loop 4.25 metres per side. The 1m by 0.5 m multi-turn receiver coil (Rx1) is the waterproofed upper coil of the EM61-MK2. A standard Geonics underwater coil (Rx2) was also mobilized in Phase IV to help diagnose noise problems and was used for some of the tests.

The MK2 system has two transmitter power settings, low (LP) and high (HP). The details of the timing of excitation pulse and receiver channels are provided in Appendix A, summarized in Table 2 and shown schematically in Figure 1. Several points regarding the system are worth noting.

The time gates delays are the same in both high and low power relative to the peak current (start of the decay ramp). However, with the additional current draw (4/3 times normal) of the large transmitter the position relative to end of the ramp and the powering pulse changes. In the Results section below we will see that the change in position of the time gates relative to the end of the signal appears to have significantly influenced the response of the system in low and high power.

Table 2: Timing (in usec) of receiver channels for Geonics EM61 MK2HP (refer to Appendix A for additional details) Note: the large transmitter loop draws approximately 4/3 times the amperage of a standard transmitter, which will affect the decay ramp and the position of the time gates relative to the end of the transmitter pulse.

Low Power

Max Current 6.02 A (@ 12.39V battery input
Relative to Current off (56 usec after peak)

Channel	Start	Center	Duration
1	267	317	100
2	366	432	131
3	497	583	172
4	669	782	226

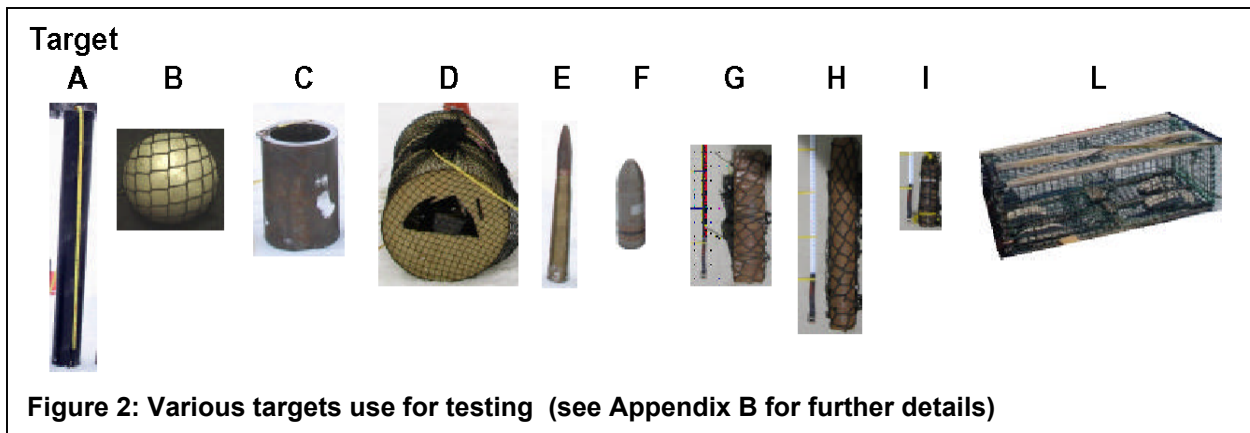
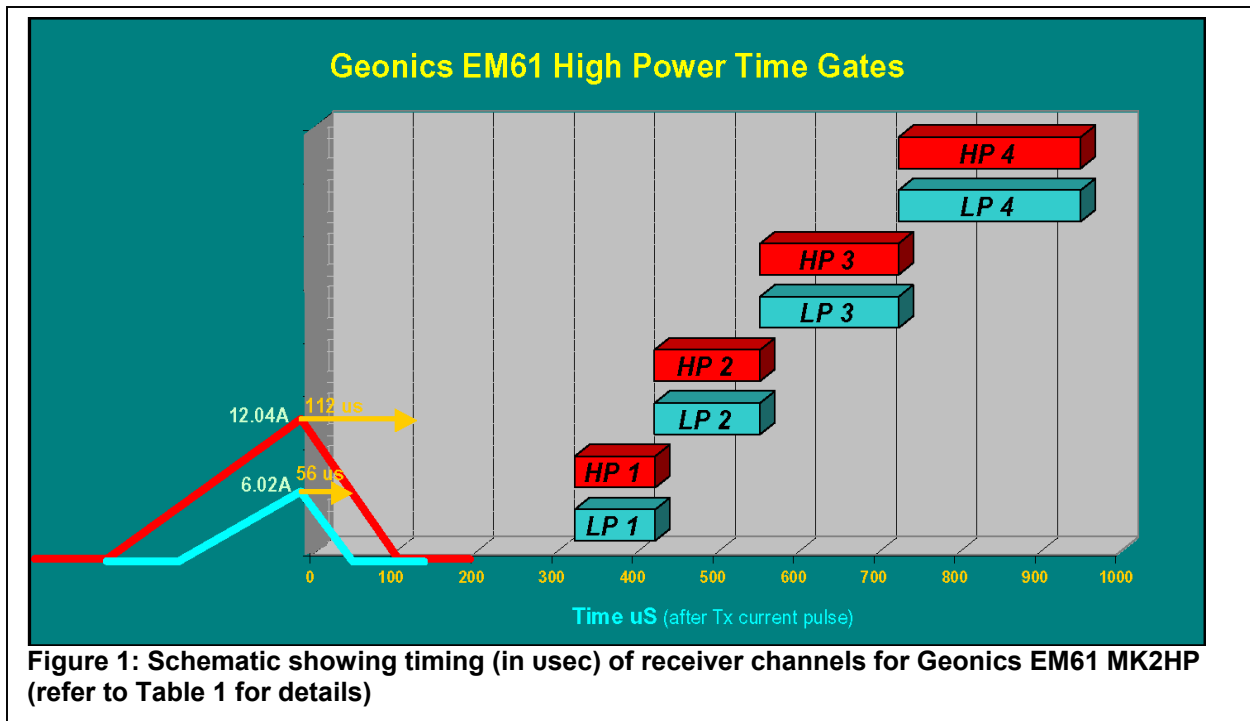
High Power

Max Current 12.04 A (@ 12.39V battery input)
Relative to Current off (120 usec after peak)

Channel	Start	Center	Duration
1	211	261	100
2	310	376	131
3	441	527	172
4	613	726	226

In the high power mode the system should provide twice the energy output of the low power mode. The instrument internally halves the high power readings providing a similar level of response and theoretically lower noise levels. We therefore anticipate twice the signal to noise ratio from the high power mode.

The MKII system has an internal system that compensates for the decreasing power output from the transmitter as the energy from the battery deteriorates. Essentially the internal gain of the system is increased to provide a constant output. Note that this process will slightly increase the noise (decrease the signal/noise) when battery power fades as the survey progresses. The maximum change is approximately 30 percent (M. Bosner pers. comm.). The system with a large transmitter coil draws approximately 4/3 more power than does a standard coil. We now suspect that the software monitoring and compensation for decreasing battery power may have mistakenly treated some of our low power data as if it were high power data with inadequate battery power. This may account for some of the offsets occasionally observed in the data.



2.4 Targets

Targets designed to simulate ordnance were collected and/or fabricated. We chose targets that were comparable to some of those used by ECC for comparing technologies at Mare Island. A 45- gallon (imp) drum and a lobster trap were used as examples of scrap metal since these are plausible non-ordnance metal objects that could be encountered. The details of the target suite are included as Appendix B.

2.5 Deployment

The survey began with choosing a location that provided sufficient water depth ($\geq 16\text{m}$). The bottom was checked for metal using a borehole video camera and a Geonics EM39 electrical conductivity logging tool.

For Phase I a rectangular hole slightly larger than 1 x ½ metre receiver coil was cut in the ice (.45m thick). (Figure 3a), A wooden control frame was centred about the hole and nailed into the ice surface and the receiver lowered through the frame and secured at the required depth. Finally the transmitter loop was placed on the ice surface, centred over the receiver coil. Electronics, targets and other metallic objects associated with the test were placed at least 10 metres from the edge of the transmitter coil.

Phases II through IV were conducted on open water using the plastic barge normally used for deployment as a platform (shown schematically in Figure 3b and in Figure 3c) The receiver coil, wooden frame, beam for lowering targets were normally centred for most of the tests.

The water surface, nominally 10 cm below the transmitter coil, was used as a reference point for depth measurements. Lateral measurements were referenced to the centre of the receiver coil, using an X (easting), Y(northing) coordinate system.



Figure 3a: Phase I testing set up

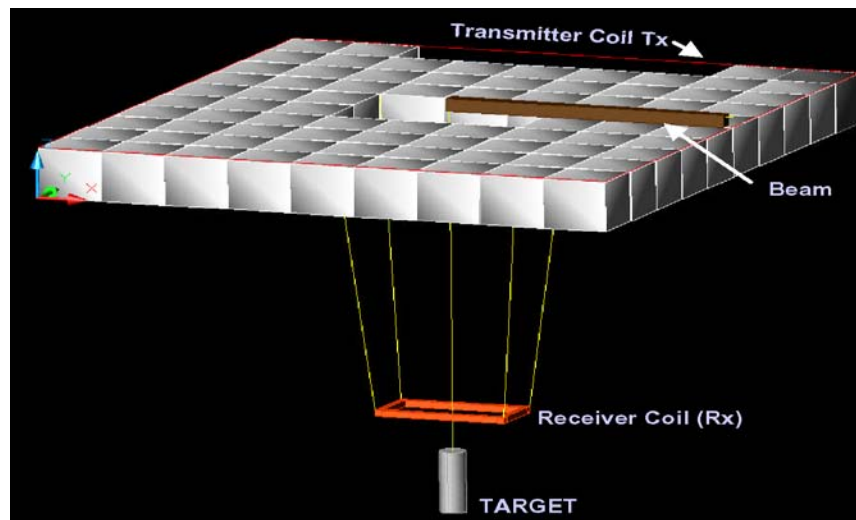


Figure 3b: Schematic of equipment deployment



Figure 3c: Photo of Phase IV geometry testing (Note Rx and target are not centred for this test)

Centred response tests for an ordinance would typically involve setting the receiver coil at a specific depth (“receiver depth”) below the transmitter and lowering the target down from the middle of receiver. The targets were placed in nets and a tape measure attached to the top of the target. The term “target depth” refers to the distance from the water surface to the top of the target. When the symmetry of the target was such that its orientation had no potential bearing on the readings, the object was lowered using a single centred tether. However if the orientation of the target could have some bearing on the receiver response, for example for an artillery shell in horizontal position, a measured tether was attached to either end of the suspended object.

The water conductivity was also logged with the EM39.

2.6 Specific Tests

The tests conducted in each phase of the project are summarized in Appendix A-3. The tests are grouped according to the specific purpose as shown in Table 3.

Table 3: Description of various tests

Test	Receiver Rx			Target			Comment
	Geo.	Depth	Orien.	Type	Geo.	Depth	
Background	Centred	Various	Horiz.	None/B	Centred	2,4 & 6	Target not always used
Decay	Centred	Various	Horiz.	Various	Centred	Various	
Alignment	Centred	2,4 & 6	Tilted	B	Centred	Various	
Geometry	Various		Horiz.	A&B		Various	
Tx signal variation	Various	2,4 & 6	Horiz.	A&B	Centred	Various	
Negative	Various	2,4 & 6	Horiz.	A&B	Various	Various	Polarity reversals in response
Transmitter	Centred		Horiz.	B	Centred	Various	
Orien.	Orientation – Rx alignment to horizontal						
Geo.	Geometry – relative horizontal position of Rx to Tx, & target to Rx						

Most, but not all tests were done in both salt and freshwater. A limited number of tests were conducted more than once to assess repeatability.

2.7 Data Processing

The operating procedure specified by the manufacturer (Geonics Limited, 2005) calls for the system to be initially allowed to stabilize and then to be nulled over an area with no metal present (background). Simply, the nulling procedure averages the system output at a particular (short) period in time, given the condition (coil geometry, batteries etc) and the local environment (geology, temperature, EM noise etc.), and assigns the value recorded for each channel to be “zero”. Variations in instrument response (positive and negative) from that point until the system is re-nulled are now referred to that “zero”.

The background null (or zero) of the Geonics MK2 system has a tendency to change slightly over time (see below). The rate of this drift appears to increase as battery power wanes. This drift can be simply removed when processing normal survey data by normalizing (subtracting) the low frequency variation.

Ideally the system would be nulled every time the geometry of the coils changes. However nulling prior to each individual test is a time consuming process, and the benefit of the nulling process is often negated by the time dependant drift. We adopted a post-processing nulling procedure wherein after an initial nulling is completed for a series of tests, the average values of a window of data not under the influence of the target is used to provide a correction factor for each individual test. An example of the nulling the data in the post processing is provided in Table 4.

This process essentially provides a moving average over time, analogous to the process that would be applied to normal survey data. Background tests (see below) showed that when the separation of the Rx and Tx is beyond a metre, the influence of geometry on the readings is minimal and therefore the corrections applied would be fairly small for most of the data.

During the various phases of this project, the polarity of the response to the targets would be either negative or positive depending on the orientation of the transmitter loop. The polarity is reversed by flipping the transmitter loop or by interchanging its connections to the current source. For convenience all data in this report are shown as positive. No other adjustments, filters or interpolations were applied to the data. All estimates of variability based on standard deviations in the results remain unaffected by this process.

Table 4: Example of correction applied to data from one decay curve test for Target C. Rx is at 1m. Prior to test nulling had been completed with Rx at 5m and target at 20m. To null the data in post processing the average for each channel of the shaded values is removed to create the “nulled” data. The depth referenced is changed from the receiver to the water surface.

RAW DATA					NULLED & DEPTH CORRECTED DATA				
Depth Below Rx	Ch 1	Ch 2	Ch 3	Ch 4	Depth Below Surface	Ch 1	Ch 2	Ch 3	Ch 4
0	12530.42	9677.51	7250.6	6018.1	-1	12517.24	9664.66	7242.27	6011.34
0.2	5794.6	4422.73	3299.18	2710.43	-1.2	5781.42	4409.88	3290.85	2703.67
0.4	2701.94	2058.25	1524.4	1270.27	-1.4	2688.76	2045.40	1516.07	1263.51
0.6	1329.22	1012.53	756.41	632.63	-1.6	1316.04	999.68	748.08	625.87
0.8	707.23	548.29	411.04	344.2	-1.8	694.05	535.44	402.71	337.44
1	412.07	321.15	239.89	201.28	-2	398.89	308.30	231.56	194.52
1.2	256	200.57	149.75	125.76	-2.2	242.82	187.72	141.42	119.00
1.4	166.94	131.95	98.26	82.55	-2.4	153.76	119.10	89.93	75.79
1.6	115.65	92.11	68.37	57.35	-2.6	102.47	79.26	60.04	50.59
1.8	81.74	65.54	48.51	40.66	-2.8	68.56	52.69	40.18	33.90
2	61.36	49.86	36.59	30.88	-3	48.18	37.01	28.26	24.12
2.2	48.98	40.29	29.4	24.5	-3.2	35.80	27.44	21.07	17.74
2.4	38.55	32.43	23.4	19.7	-3.4	25.37	19.58	15.07	12.94
2.6	32.09	27.46	19.46	16.51	-3.6	18.91	14.61	11.13	9.75
2.8	26.98	23.38	16.52	14.02	-3.8	13.80	10.53	8.19	7.26
3	23.47	21.01	14.45	12.07	-4	10.29	8.16	6.12	5.31
3.2	21.27	18.86	13.03	11.01	-4.2	8.09	6.01	4.70	4.25
3.4	19.01	17.45	12.05	9.77	-4.4	5.83	4.60	3.72	3.01
3.6	17.85	16.27	11.08	9.24	-4.6	4.67	3.42	2.75	2.48
3.8	16.49	15.38	10.21	8.71	-4.8	3.31	2.53	1.88	1.95
4	15.72	14.78	9.99	8.36	-5	2.54	1.93	1.66	1.60
4.2	14.96	14.41	9.23	7.82	-5.2	1.78	1.56	0.90	1.06
4.4	14.47	13.89	9.22	7.64	-5.4	1.29	1.04	0.89	0.88
4.6	14.42	13.51	8.81	7.48	-5.6	1.24	0.66	0.48	0.72
4.8	13.59	13.59	8.7	7.3	-5.8	0.41	0.74	0.37	0.54
5	13.51	13.36	8.7	6.94	-6	0.33	0.51	0.37	0.18
5.2	13.33	13.07	8.46	6.93	-6.2	0.15	0.22	0.13	0.17
5.4	13.12	12.78	8.46	6.76	-6.4	-0.06	-0.07	0.13	0.00
5.6	13.12	12.7	8.24	6.76	-6.6	-0.06	-0.15	-0.09	0.00
5.8	13.06	12.7	8.02	6.58	-6.8	-0.12	-0.15	-0.32	-0.18
6	12.96	12.48	8.13	6.58	-7	-0.22	-0.37	-0.20	-0.18

Average Ch 1=13.18 Ch2=12.85 Ch 3=8.34 Ch4 = 6.76

3.0 RESULTS AND ACCOMPLISHMENTS

3.1 Water Conductivity

The electrical conductivity – depth structure for the Phase I and IV surveys in Bay’s Lake are shown in Figure 4. The average water conductivity is shown to be 2.5 mS/m in the winter (Phase I) and 12.7 mS/m in the fall (Phase IV). The overall increase in conductivity presumably results from the change in temperature, larger seasonal watershed variations (suspended solids, runoff etc.) and the fact that the tests were conducted in slightly different parts of the lake.

Based on the sediment returned to the surface on targets that temporarily sat on the bottom, the lakebed surface is a silty clay. The increasing conductivity values slightly above the lake bottom presumably result from the fine-grained sediment and some minimal water disturbance. At surface the effect of the ice is apparent in the Phase I test and the late summer heating in the Phase IV test.

The water conductivity in the marine environment was beyond the dynamic range of the EM39. Water conductivity was measured from samples collected at the bottom of the water column and at the water surface. Conductivity ranged from 8500 mS/m at the surface to 3400 mS/m at depth. The bulk of the water column is estimated to have had a conductivity of about 3500 mS/m at the time of the test.

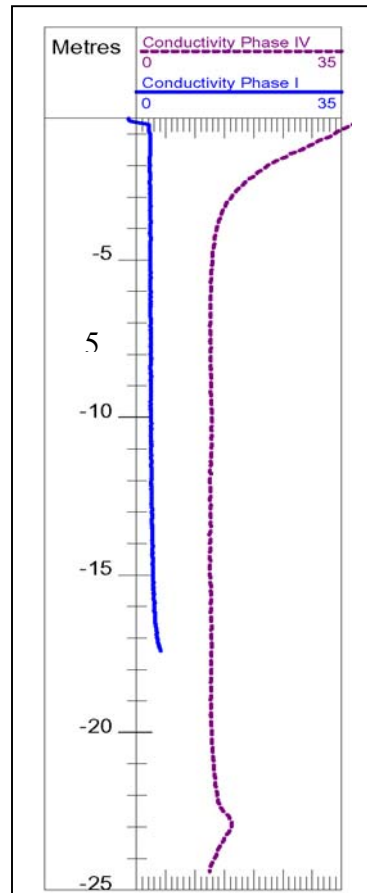
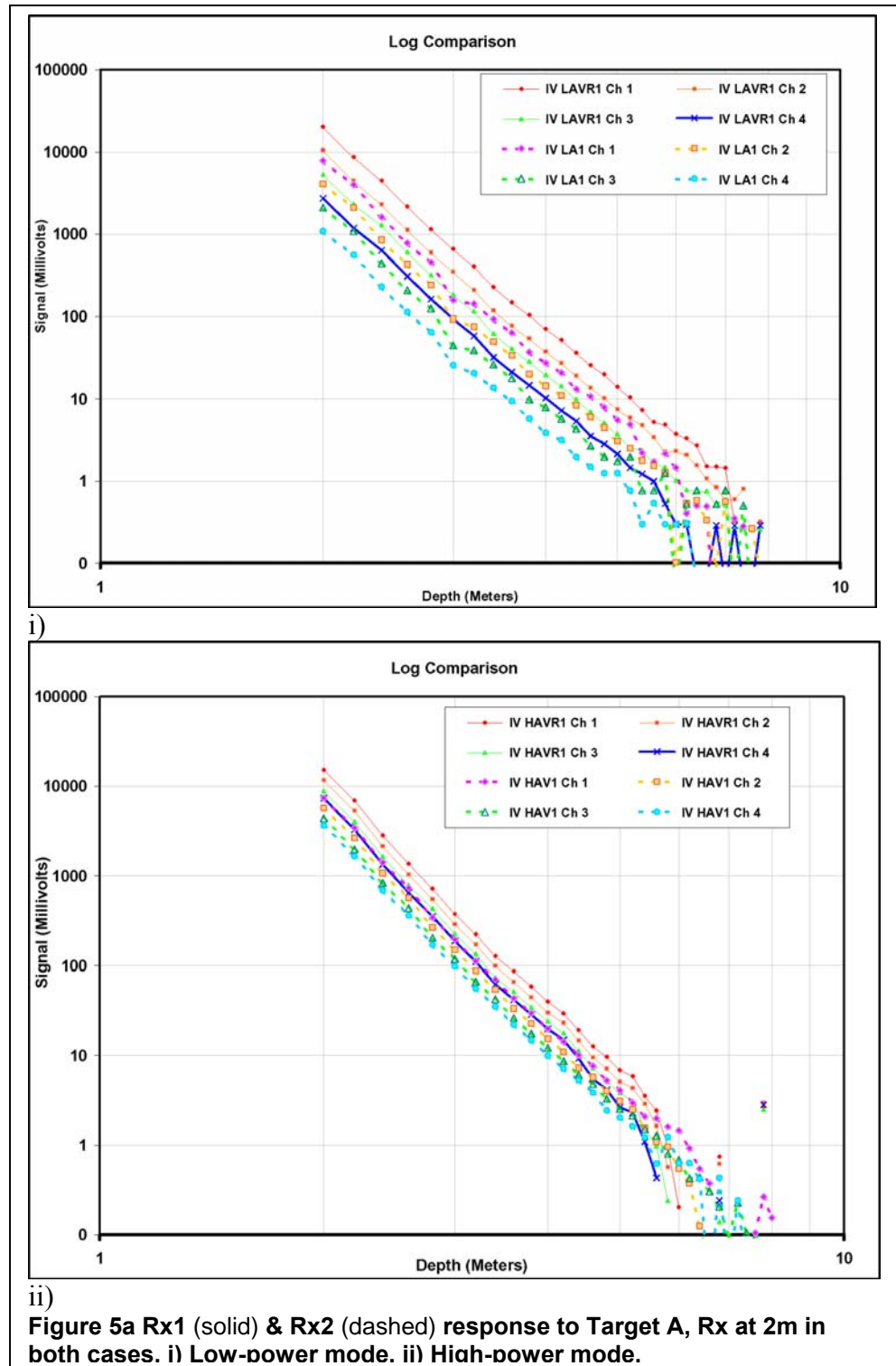


**Figure 4: EM39
Conductivity profile
through water column**

3.2 System Variability

3.2.1 Rx1 vs. Rx2

The majority of the tests were conducted with the underwater receiver coil built specially for DCL, which we have designated as Rx1. When noise issues were identified (see above), portions of the testing were conducted using a standard Geonics underwater coil (Rx2). An interim method of reducing the noise in Rx1 was devised that provided better electrical isolation between the receiver and the transmitter. Figure 5a compares the output of Rx1 and Rx2 for Target A. The responses are similar but offset. The output of the coils changes with the power setting of the instrument. The average percentage differences between the two receiver responses for low and high power transmitters are summarized in Table 5.



i)

ii)

Figure 5a Rx1 (solid) & Rx2 (dashed) response to Target A, Rx at 2m in both cases. i) Low-power mode. ii) High-power mode.

The values observed with the system set at high power are consistent with Rx2 having half the windings of Rx1. The observed values in low power mode are not winding-consistent, suggesting that factors such as the position of the gates in time relative to the end of the primary pulse may have an influence (see below).

Table 5: Rx2 response as a percentage of Rx1

	CH 1	CH 2	CH 3	CH 4
LP	37.6%	38.6%	37.5%	38.9%
HP	50.6%	51.1%	51.2%	51.8%

Figure 5b provides another comparison of Rx 1 and Rx 2. The data were collected in Phase IV (with noise reduction for RX1 implemented). The figure compares the standard deviations observed with the two receiver coils at various depths and target B at 1metre below the Rx coil. These data show that the Rx 1 response is consistently more variable than the response of Rx 2. The dashed line shows the 2:1 ratio high-powered instrument response from Table 5. Therefore, although the Rx1 output is more variable in its current condition it still provides a better signal to noise ratio than does Rx2. Since Rx1 had a

temporary noise suppression rather than the permanent hardware correction, those ratios can be expected to improve in favour of Rx1.

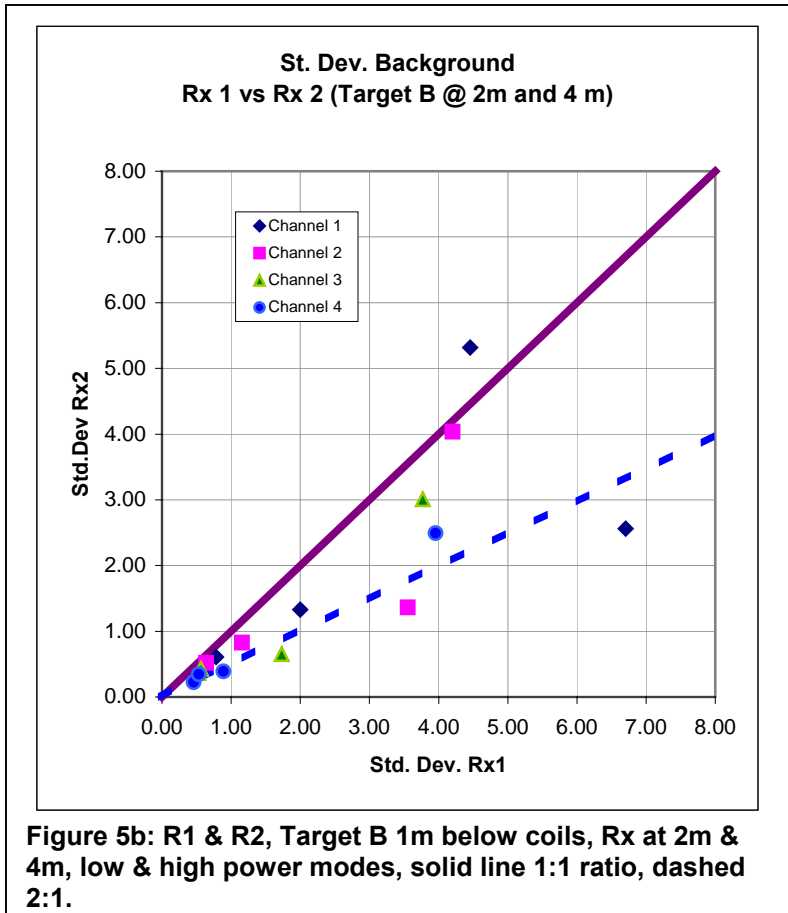


Figure 5b: R1 & R2, Target B 1m below coils, Rx at 2m & 4m, low & high power modes, solid line 1:1 ratio, dashed 2:1.

3.2.2 Low vs. High Power

Figure 5a also highlights the difference between high and low power modes. The range of values between channels 1 and 4 observed with the instrument set at low power is considerably broader than that observed with the instrument set on high power.

Figure 6 directly compares the instrument response in low and high power modes to target A with Rx2 set at 2 metres. The first (early time gate) channels provide similar values in both modes. The later gates in low power have progressively lower response than are observed in high power. Recall that the output of the high power

mode is divided in half by the data logging software².

² Note newer versions of the MK2 console do not divide HP readings in half, but provide the response as measured, in which case the signal is twice as strong and the noise would be the same.

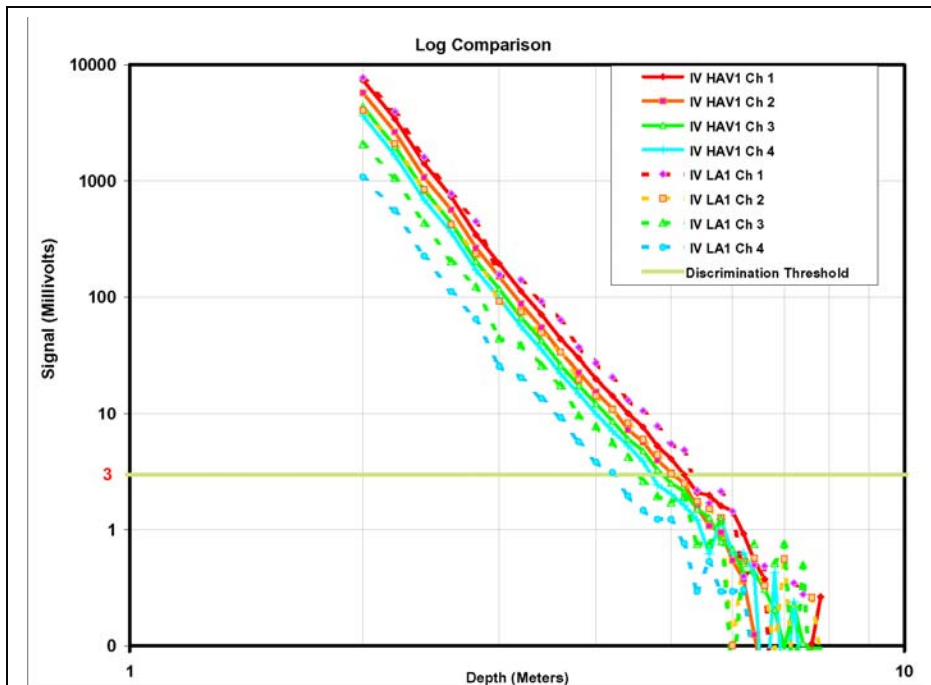


Figure 6: Low (dashed) vs High Power (solid) Decay, R2 at 2m, Target A

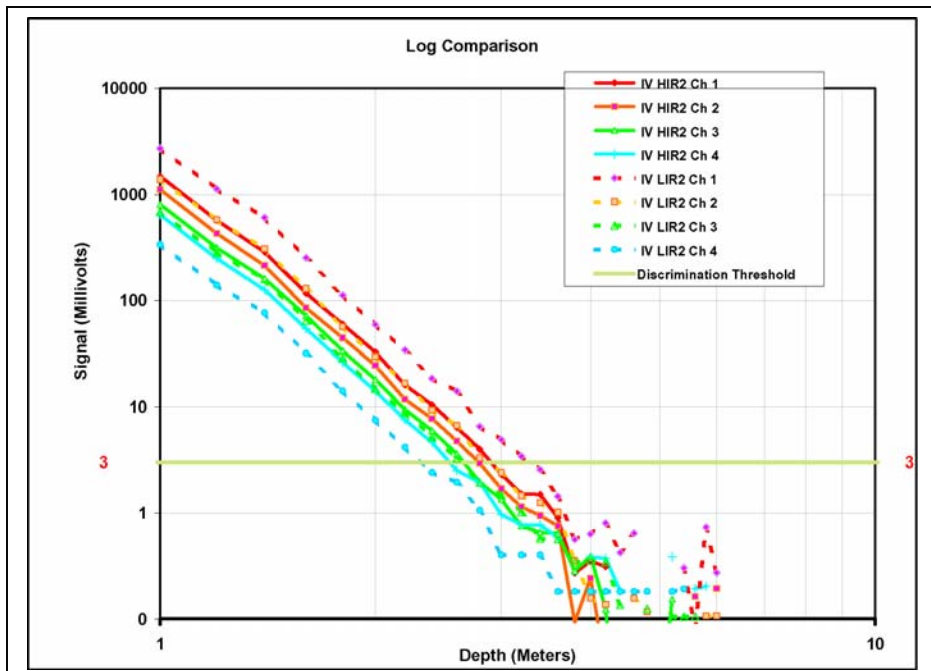


Figure 7 Low (dashed) vs High (solid) Power Decay, R2 at 1m, Target I

The implication of the “signal spreading” in low power mode is that if the span (over time) of the sampling gates is the same in both modes, then the sampling must be occurring at a different portion of the target’s decay curve. Since the values in all channels approach zero with time, the low power mode must be measuring relatively earlier in the decay curve.

The response ratios between high and low power are not consistent, varying with the target. Figure 7 compares the low and high power modes for target I. In this case although the relative “spread” of that data is similar to Figure 6, the high power mode values plot in the middle of the low power response with channel 2 values overlapping.

The relative “spread” in the data between high and low power is independent of water

conductivity, target, transmitter (see below) or the receiver coil used. Testing by Geonics (M. Bosner pers. comm.) has indicated that the low and high power responses are the same when the standard MK2 coils are used on land. This implies that the spreading is peculiar to the Rx/Tx combination used here.

3.3 Background Variability

Every geophysical system has a level of background “noise” or variability against which the instrument response to a target must be compared. Figure 8a graphs the Rx1 response recorded at 10 samples per second over a period of approximately 2 minutes with the receiver coil set 5 metres below the transmitter, without a target. Figure 8b is the low power response for Rx1 at 4m with target B (aluminium ball) 1 metre below the coil. Figure 8c shows the same information as 8b, but in high power mode. Note that in each figure the data channels have been offset to make the responses easier to differentiate. The variability (standard deviations) of the responses over the data provided in Figure 8 are summarized in Table 6.

Table 6: Background variability, standard deviation values for Figure 8.

Example	Standard Deviation			
	Ch1	Ch2	Ch3	Ch4
A- Low power, no target	0.372	0.307	0.229	0.240
B- Low power, target	6.780	3.440	1.649	0.861
C- High power, target	0.781	0.639	0.527	0.531

See text and Figure 8 for details of tests.

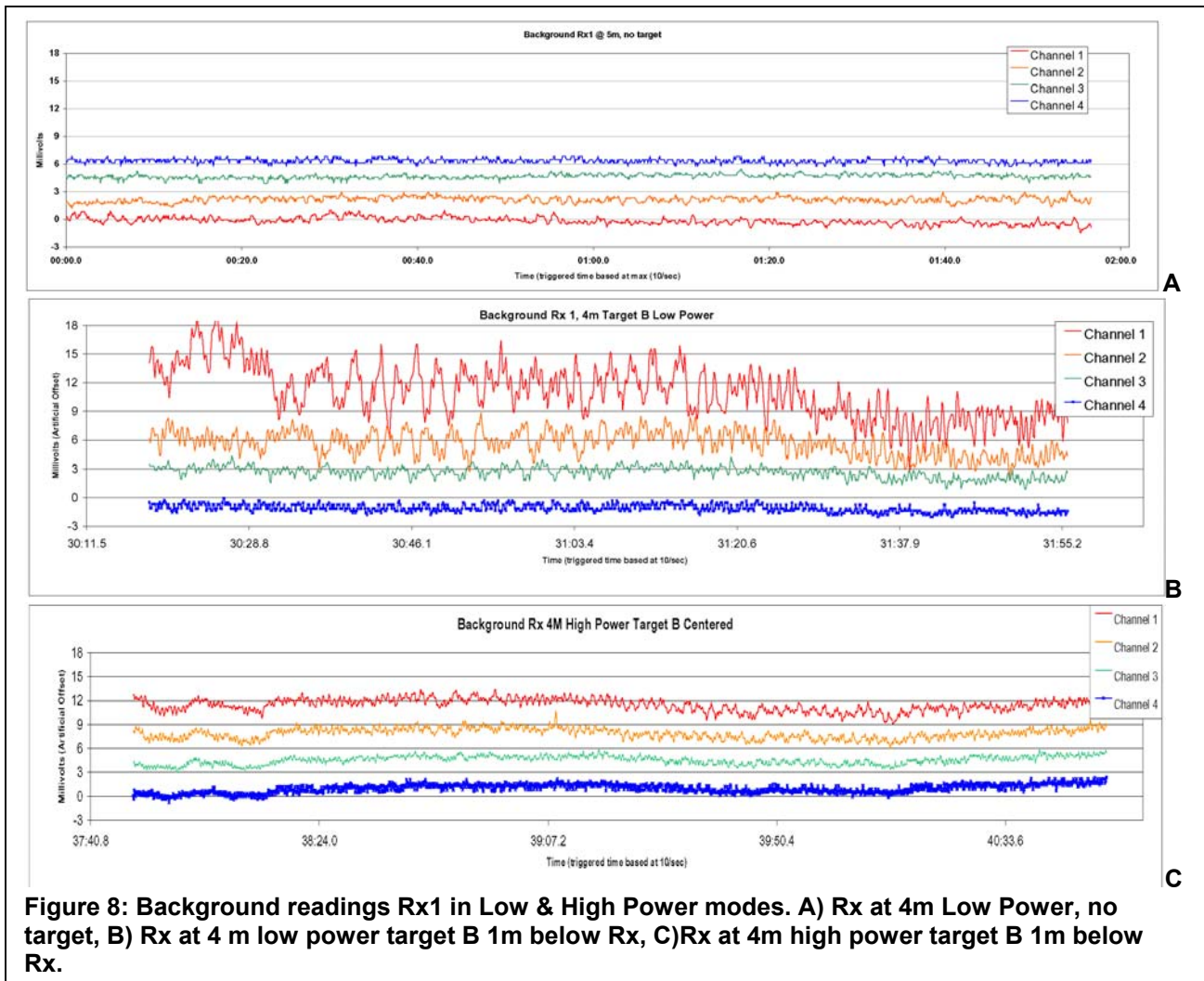


Figure 8: Background readings Rx1 in Low & High Power modes. A) Rx at 4m Low Power, no target, B) Rx at 4 m low power target B 1m below Rx, C) Rx at 4m high power target B 1m below Rx.

Note that the data shown in Figure 8 are for Rx1 with interim steps taken to reduce sporadic noise. Without the noise reduction, irregular spikes that last approximately 0.4-0.6 of a second in Channel 1, and are narrower as well as smaller in the later channels, dominate the high power response. The spikes could easily be mistaken for an anomaly and must be corrected. The tests conducted using the instrument in low power mode do not show these spikes. There is also a significant, gradual drift in the background values of Channels 1 and 2. This drift could be removed in post processing and is not a crucial limitation.

The noise level with the system stationary, as measured by the standard deviation of the response about its mean without a target, are very low although marginally higher in the earlier (1&2) than the later channels. In the presence of a target noise on the early channels increases significantly, while noise on channels 3 and 4 increases only slightly. Relative motion between the target and the receiver may account for a significant portion of this variability. With the target in place,

Table 7a: Standard deviation of 60sec sampling of the low power background data at various receiver depths in salt water.

Rx Depth	Channel			
	1	2	3	4
0.0	3.2	1.4	0.7	0.5
1.0	2.9	1.3	0.7	0.6
2.0	3.2	1.4	0.7	0.4
4.0	3.0	1.3	0.6	0.5
6.0	4.6	2.2	1.2	0.9
8.0	3.6	1.6	0.9	0.8
Average	3.4	1.5	0.8	0.6

Correlation				
w. Depth	0.62	0.57	0.63	0.76
w. Channel	-0.92			

Table 7b: Standard deviation of 60sec sampling of the high power background data at various receiver depths in salt water. Note a portion of high-powered response without anomalous spikes was chosen.

Rx Depth	Channel			
	1	2	3	4
0.0	6.2	2.6	1.1	0.7
1.0	4.5	1.9	0.9	0.6
2.0	4.4	1.9	0.9	0.5
4.0	8.9	4.0	1.7	0.9
6.0	6.9	3.7	2.5	2.7
8.0	10.5	5.0	2.1	1.2
10.0	18.8	9.5	3.9	2.4
Average	8.6	4.1	1.9	1.3

Correlation				
w Depth	0.85	0.88	0.91	0.75
w. Channel	-0.94			

measurements using high power mode vary significantly less than in the low power mode. If the noise is a function of the position of the time gates relative to the excitation pulse, this observation implies that the low power mode is measuring earlier in the decay curve.

To examine the variability of the system with changing geometry we tabulate the standard deviation in background mode (no target) with varying Rx1 depths in Table 7a for low power and 7b for high power. These data are taken from readings taken in saltwater and are graphed in Figures 9a and 9b respectively.

In the low power mode correlation is low between the variability of the background reading and the depth of the receiver. There is however a strong correlation between the standard deviation and the time channel used, with the early channels being the most variable. Note that the standard deviation values in Table 7 are distinctly higher than those presented in Table 6. The source of this noise had yet to be identified and noise reduction measures were not implemented

for the data in Table 7. Therefore establishing whether the differences in variability result from the water conductivity (fresh water vs. marine) or the noise reduction measures is unresolved from this data.

The increase in standard deviation with receiver depth implies that this contribution to the noise is not directly related to the transmitter. Given the increased power draw in high power mode, a contributing factor could be the system's method of compensating for decreasing battery voltage by automatically increasing the internal gain settings. Increasing the gain will also have the apparent effect of increasing the noise levels. This compensation should not be large enough to explain the magnitude of the increase in noise. A more significant contributing factor could result from the decreasing rigidity of the receiver coil as it is lowered progressively deeper. Movement of the coil through the earth's magnetic field can have a significant contribution to background noise (M. Bosner pers. comm.). These results have practical implications for system deployment and the interpretation of the data, as discussed below.

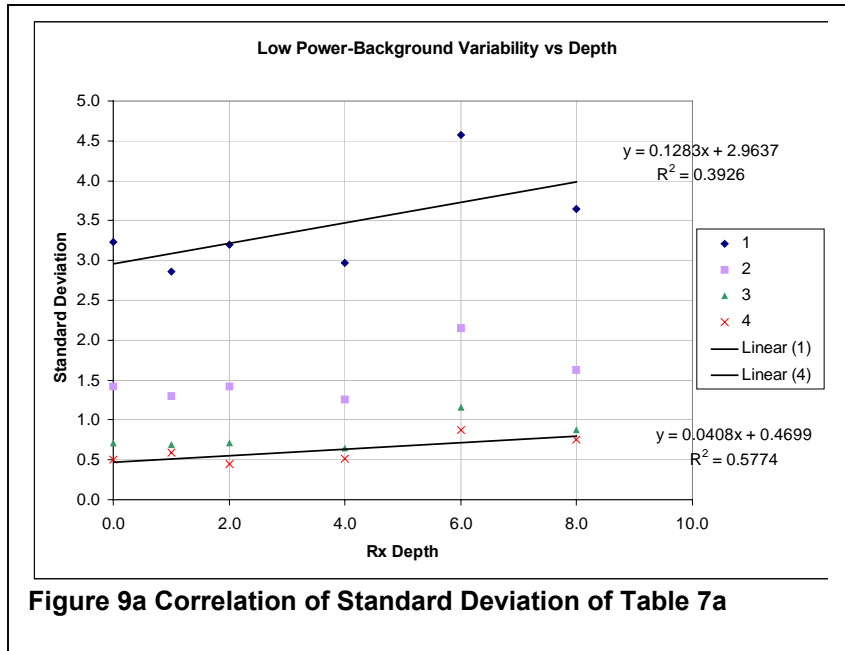


Figure 9a Correlation of Standard Deviation of Table 7a

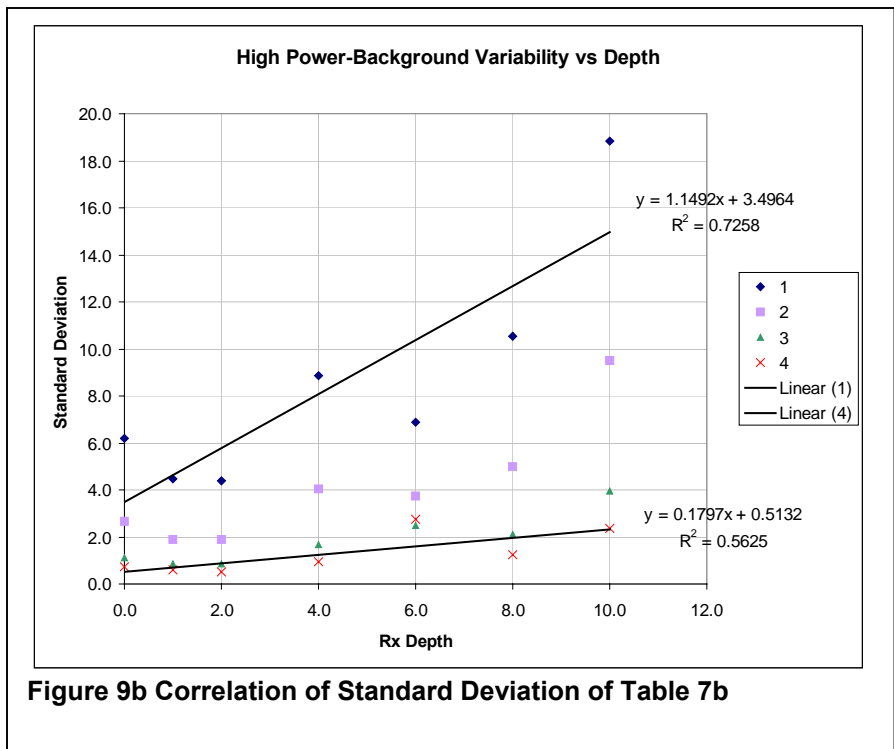


Figure 9b Correlation of Standard Deviation of Table 7b

In high power mode, there is good correlation of the standard deviation with both the channel being measured and receiver depth. The correlation with the channel is similar to that observed in low power, with a similar rationale for its existence.

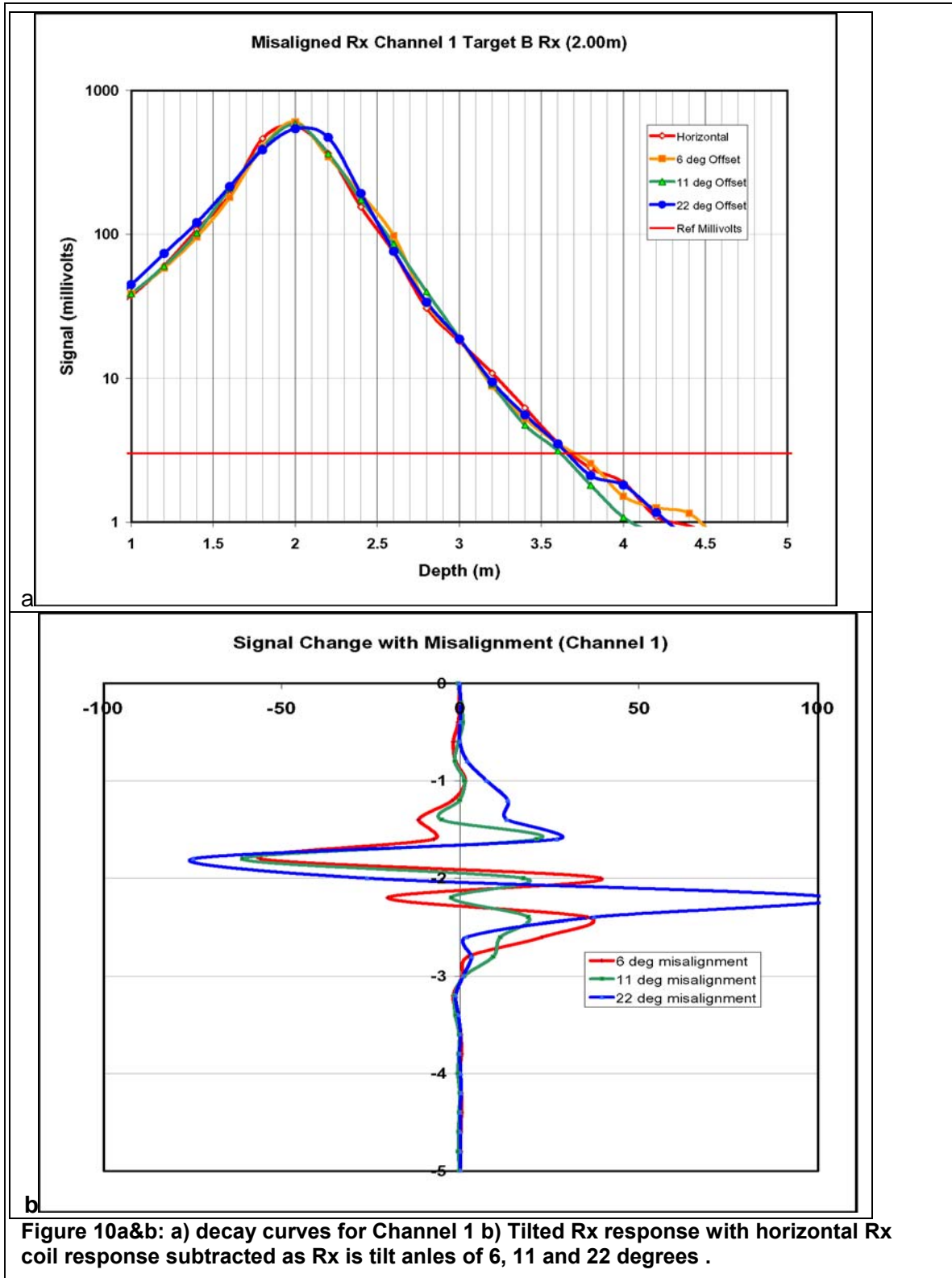
3.4 Geometric Variability

The scope of this project deals with the system and its variability under stationary conditions. The noise levels are shown to be below 2 millivolts when the system is not moving. To examine the potential for response variability that could occur while under way, the alignment of the receiver coil was systematically varied and decay curves were measured. The procedure involved tilting the receiver coil by raising one end of the long dimension by 0.05 metres while lowering the other end the same distance (a total end-to-end tilt of 0.1 metres or 6 degrees). A decay curve was measured from surface through the receiver beyond detection below. The process was then repeated for end-to-end tilts of 0.2 and 0.4 metres (11 and 22 degrees respectively).

When the receiver was tilted from the horizontal in the absence of a target no increase in the “background” noise levels was observed. Figure 10a&b compare the results of this process against the response from a horizontal coil for target B in two ways. Figure 10a shows the decay curves. The horizontal line at 3 millivolts represents minimum signal above background required for detection. Figure 10b shows the decay data with the horizontal response subtracted as a function of depth and tilt angle on a linear scale. In this case the system is in fresh water, in high power mode, and the receiver nominally set 2 metres below the transmitter. Channel 1 data are shown in Figure 10a because it is the most variable of the channels and therefore provides the most conservative indicator.

The data (Figure 10a) indicate that for Target B detection is achieved to a target depth of 3.5 metres (1.5m below the receiver), The differences with the horizontal response are only notable above 3 meters. Although these variations are generally consistent with the expected cosine errors of .5%, 2% and 7% for the three tilt angles used, the amount and polarity of the difference varies. Tests conducted with target B in low power mode provide similar results. Similar results were obtained for target A, with detection to a target depth of 5.5m.

These results show that misalignment of the receiver up to 20 degrees have no significant effect on the ability to detect a target. It is possible, however, that these small errors could influence the ability to discriminate between two types of targets.



3.5 Lateral Response Variation Below the Transmitter

Another potential variation in the system geometry that is strictly controlled in these stationary tests is the lateral position of the receiver relative to the transmitter. It is a relatively simple matter to keep the positions stable and centred during stationary tests but controlling geometry is considerably more problematic when towing the system.

To assess the potential variation in response as the Rx coil moves laterally relative to the centre line of the transmitter, decay curves were measured using Target B and several Rx/Tx offsets. In each case the receiver was located at various locations in one quadrant below (2,4 and 6m) the transmitter (Figure 11). The target was lowered from surface through the receiver.

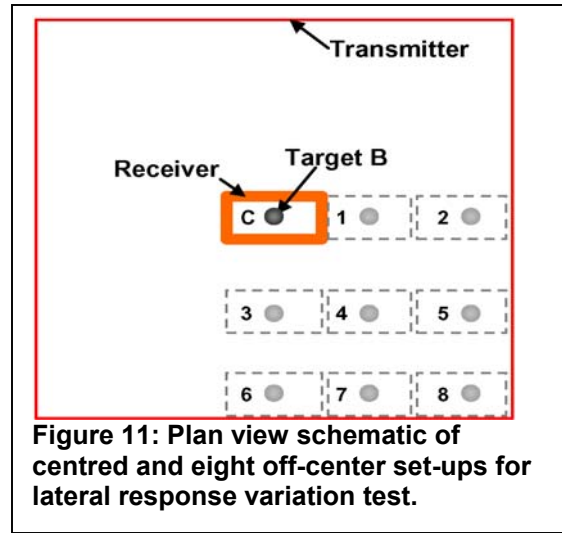


Figure 11: Plan view schematic of centred and eight off-center set-ups for lateral response variation test.

Figure 12a shows the lateral variation in channel 1 for a target 1.4 metres below the receiver (with Rx1 2 metres below the transmitter). The theoretical symmetry of the transmitted signal is used to extrapolate the results beneath one quadrant to the other three. The results show that the receiver can be moved approximately 1 Rx coil dimension in any direction with less than 10 percent variation in the response. Along the long axis of the receiver the signal decreases to approximately 80 percent of the centre value beneath the edge of the transmitter. Along the short axis the signal beneath the transmitter edge is approximately 50 percent of the central value.

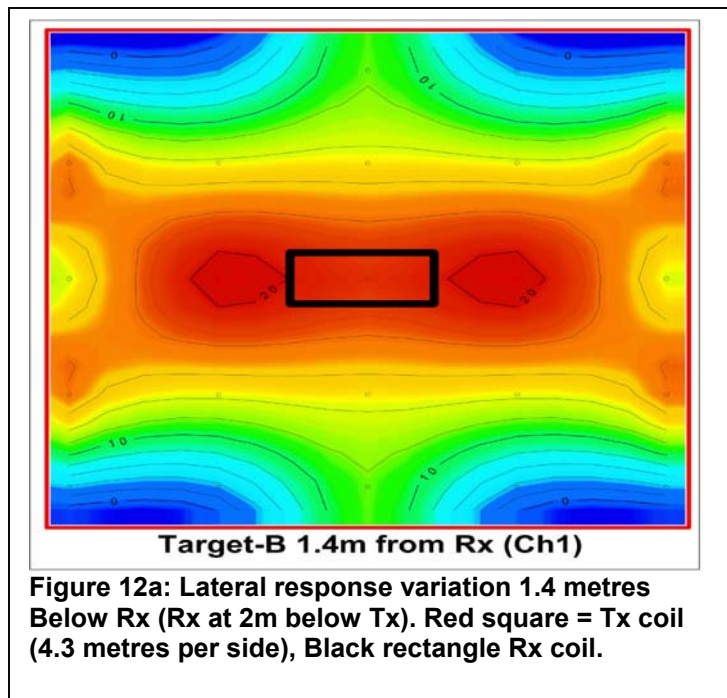


Figure 12a: Lateral response variation 1.4 metres Below Rx (Rx at 2m below Tx). Red square = Tx coil (4.3 metres per side), Black rectangle Rx coil.

An interesting phenomenon observed was that, as the receiver coil was moved away from the centre, the peak target response no longer occurred when the target was vertically centred in the plane of the receiver, but instead when it was slightly above that plane. Beneath the centre of the transmitter coil, the offset was slightly greater than 0.20 metres. If we plot the lateral variation in response as observed 1.4 metres below the peak value (as opposed to 1.4 metres below the Rx coil itself) (Figure 12b), a more symmetric pattern emerges. The variation in position of the peak value is presumably a function of the geometric coupling between Tx, Rx and target. The overall

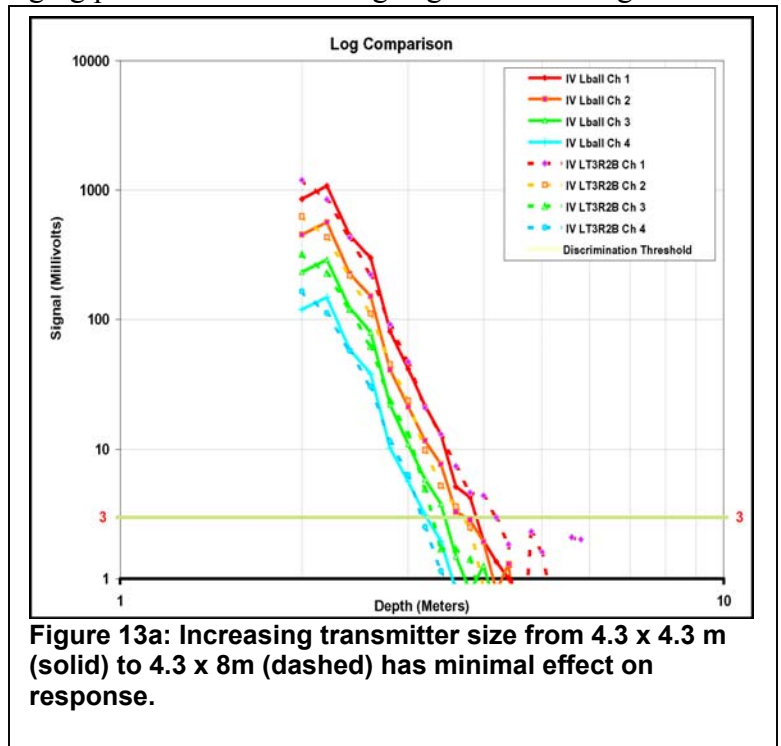
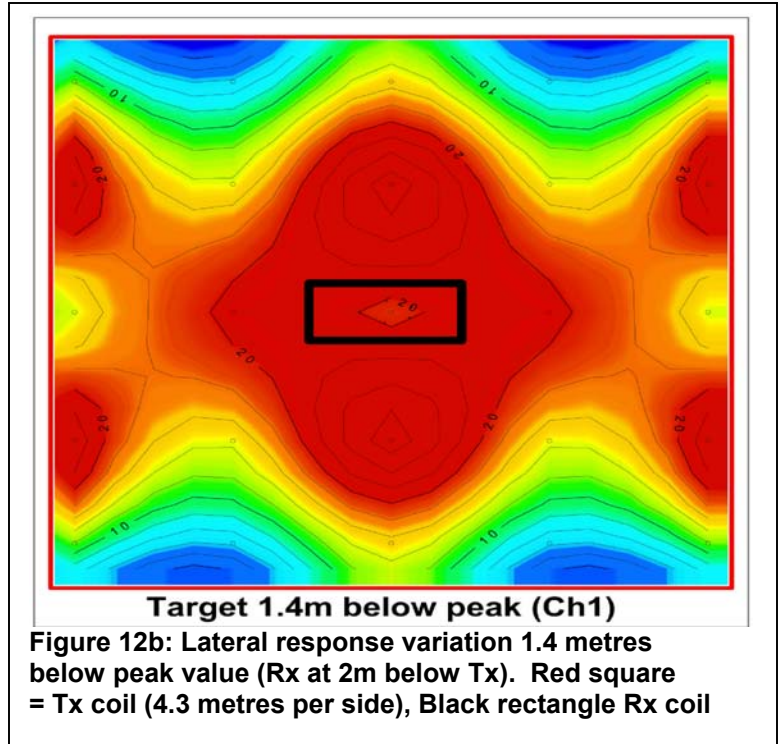
area of maximum response (“the sweet spot”, borrowing a sports analogy) is significantly larger in Figure 12b than in 12a. The centre position is actually a saddle point with slightly higher values between the long axis of the receiver and a location directly below the transmitter. This implies that the position of the receiver may not be critical to detection, a positive prospect for using multiple receiver coils and for discrimination algorithms.

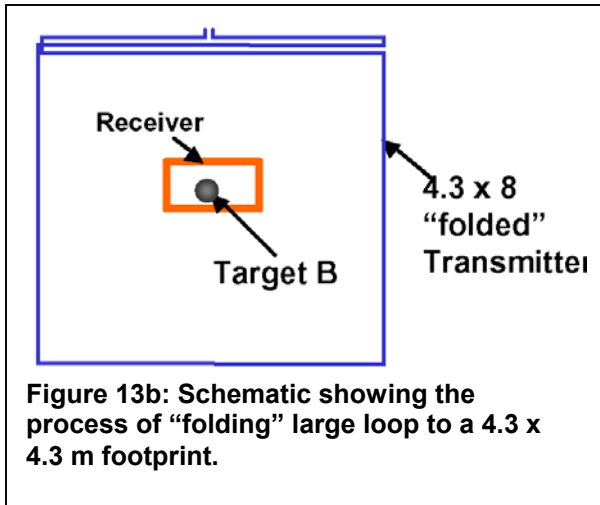
3.6 Transmitter Size

The modular nature of the barge system provides considerable flexibility with regard to overall size and shape of the transmitter. The system as originally designed was based on a compromise between “tow-ability” and the available components. The dimensions of the cubes that make up the barge control the increments with which the size of the transmitter loop can be adjusted. Experience has shown that the leading edges of the transmitter cable must be well supported on the barge with no overhanging protrusions on the leading edge while towing.

It is possible to increase the transmitter power by increasing either the loop size or the number of turns. Each choice provides it’s own compromises with regard to turn-off time (steepness of the energizing ramp) and practical deployment.

Figure 13a shows that increasing the transmitter coil from 4.3 x 4.3 m to 4.3 x 8 m has minimal effect on the response. The data are collected in freshwater using Rx2 with the receiver at 2 metres. Although the larger transmitter coil increases the strength of the primary signal, the target is also further from the transmitter wire and the benefit is offset. We expect that at a greater Rx depth some benefit of increasing the area would be observed.





We also tested the large (4.3 x 8 metre) loop with one edge of the large transmitter folded over on top of itself so that the overall footprint is still 4.3 x 4.3 metres as shown schematically in Figure 13c. Figure 13c compares the results of the "folded" and open large loop. Again the response is essentially the same for both configurations of the primary coil.

3.7 Salinity Variations

Table 9 compares the standard deviations of a sample of the background readings collected with Rx1 in Phases I, II and IV. In each case the

system is in low power mode (the most variable) and the receiver coil is either 4 or 5 metres below the transmitter. Note that for Phases I and II, the electrical noise issues associated with Rx1 were yet to be identified and no effort had been made to isolate the coil. None of the data from Phase I appears to suffer from the electrical noise issue, presumably because the coils were isolated by the almost ½ metre of ice on the surface of the water. The Phase I test has the lowest variability of the three, and it is also the test conducted in the water of lowest conductivity. What portion of the low standard deviation can be attributed to the low conductivity water and what portion to the fact that the ice isolated the transmitter and receiver coils cannot be resolved from these data. Similarly the Phase IV data have slightly lower standard deviations for channels 1 and 2 than do the Phase II data. Again the differences could be attributed to the variation in water conductivity and/or to efforts made in isolating the Rx coil.

Table 9: Standard deviation of low power background data with Rx1 at 4m (phase II & IV) and 5m (phase I). Units are mvolts.

Test	Channel			
	1	2	3	4
Salt water (II)	3.0	1.3	0.6	0.5
Fresh Water (IV)	2.1	0.9	0.6	0.4
Fresh Water/Ice (I)	0.3	0.3	0.2	0.2

The relative increases in the standard deviations with water conductivity are not consistent; although the noise in the marine environment is slightly higher than in the fresh water tests, the seawater is several orders of magnitude more conductive than the lake water. Yet the increase in variability is larger between the two freshwater phases in both absolute and relative terms.

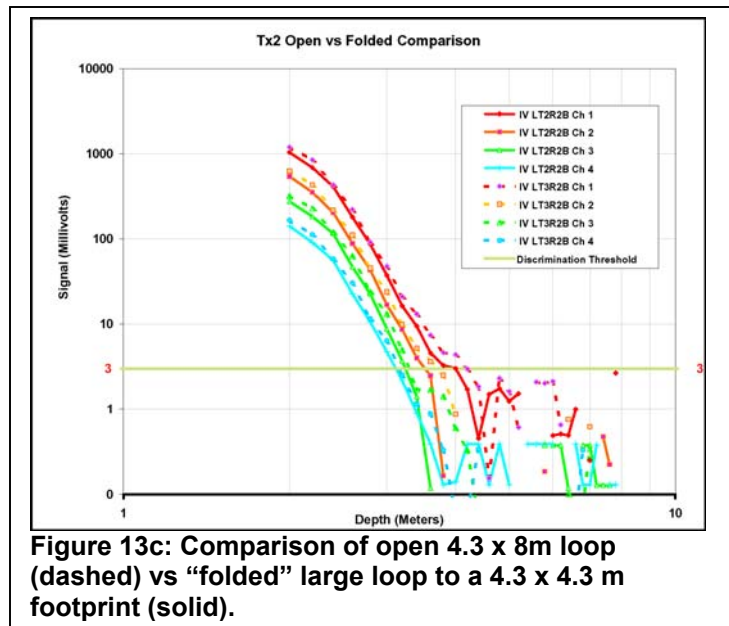


Figure 14 (a & b) compares decay curves collected for Target A in varying water salinity in low and high power modes respectively. We observe the curves for Target A in the vertical mode are essentially the same regardless of the conductivity of the water or the power mode of the instrument. The minor divergence observed in channels 1 and 2 below 4 metres is attributed to the “unsuppressed noise” in Rx1. Tests with Target A at other receiver depths had essentially the same results with some minor variability.

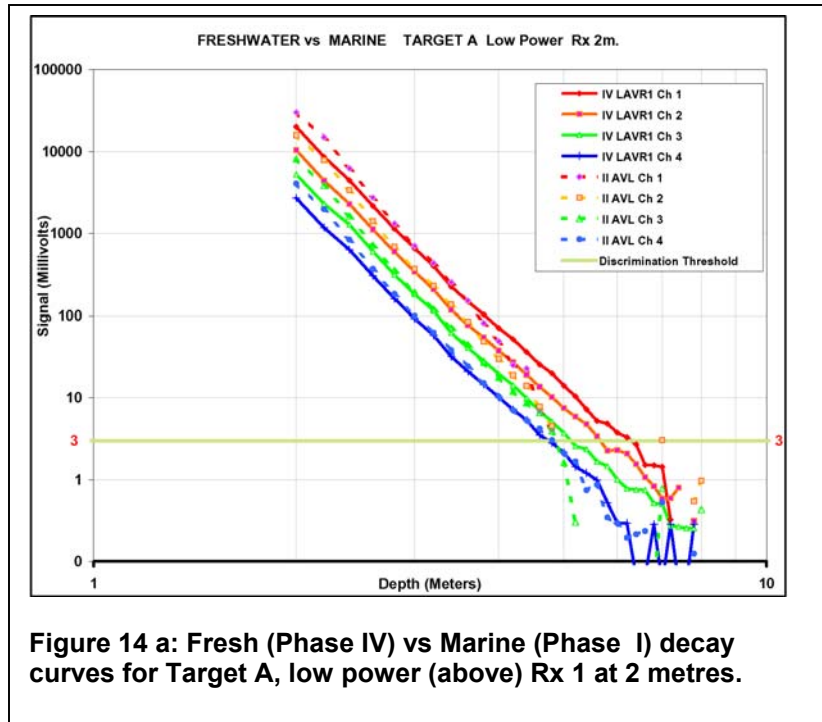


Figure 14 a: Fresh (Phase IV) vs Marine (Phase I) decay curves for Target A, low power (above) Rx 1 at 2 metres.

Figure 14c shows the decays for Target F. The saltwater responses are offset an average 30% to 35% from the freshwater. Note the minor curvature at the top of the freshwater data might imply that the data collection started too shallow, i.e. within the plane of the receiver. An upward shift of 0.35 m would be required to adjust the freshwater data to fit the marine data. With the shift, however, the correlation is excellent and the decays then have the same slope.

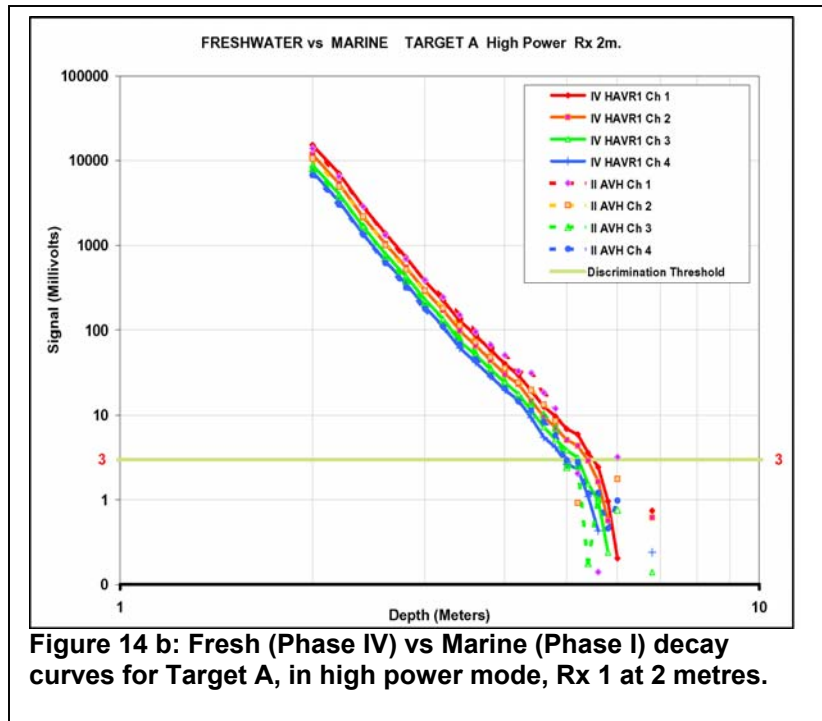


Figure 14 b: Fresh (Phase IV) vs Marine (Phase I) decay curves for Target A, in high power mode, Rx 1 at 2 metres.

The question arises as to whether this offset occurs as a result of experimental error? We note that matching the marine and freshwater responses at the water’s surface requires an

upward offset of the freshwater data by 0.1 metres, whereas the tests between 1 and 4 metres require an offset of approximately 0.35m. With the target at 6m, matching the data requires no offset. We are confident that for the data collected for the target at the water’s surface the configuration was accurately measured. Given the size of the target a 0.35m shift would move

the entire target through the plane of the coil and result in a distinct peak in the data, which is not observed. A similar response shift was observed in low power; however, the marine data in that case was on average 65% to 75% (depending on the channel) of the freshwater signal. An offset of 0.15 metres (again upwards) was required to align that data. The fact that the adjustments in all cases are upwards implies that the effect is not random, as would be expected if the phenomena originated from centring or measuring errors. The difference in the distance from the transmitter to the water surface between the phases (field measuring reference) was typically a few centimetres and does not adequately explain this response anomaly.

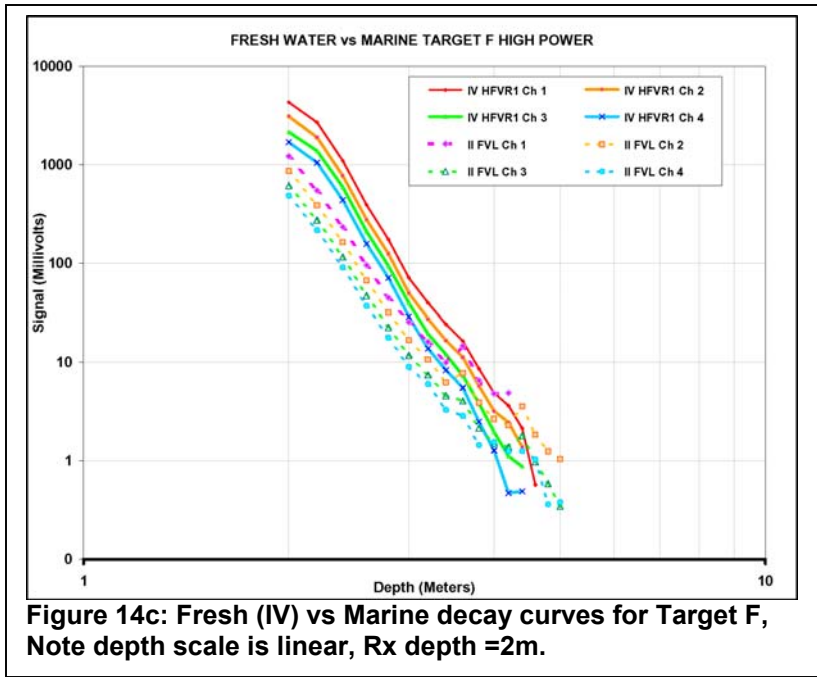


Figure 14c: Fresh (IV) vs Marine decay curves for Target F, Note depth scale is linear, Rx depth =2m.

3.8 Target Responses

Numerous examples of decay curves for targets of various sizes are provided throughout the earlier portions of this report. A complete set of decay curves is provided digitally in the Appendix. These curves all display a uniform shape (linear on a log-log plot) with the exception of those that suffer from the electrical noise issues associated with Rx1, discussed above.

3.9 Target depth-of-detection Limitations

How deep the system can detect a target depends on the Tx signal strength and the accepted threshold level of background noise. As explained earlier, we have adopted a conservative threshold of 3 millivolts for this report. We can examine the depth limitations in one of two ways.

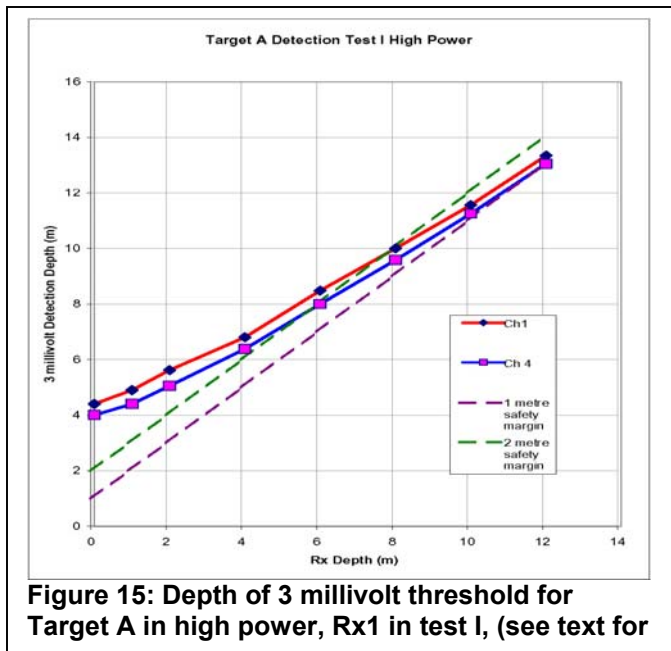


Figure 15: Depth of 3 millivolt threshold for Target A in high power, Rx1 in test I, (see text for

the depth at which Channels 1 and 4 cross the 3 millivolt threshold is noted for each decay curve and plotted against the depth of the receiver coil. At some Rx depth the line ends when there is no signal above 3 millivolts.

When determining detection limits we must also consider the height at which the receiver is “flown” above the bottom. Figure 15 includes two dashed lines, the purple representing a depth of 1 metre and the green 2 metres below the receiver. Based on the 3 millivolt threshold and a receiver height of 2 m above the bottom we can expect to detect Target A (sitting on the bottom) to a maximum depth of between 5 and 6 metres using Channel 4, and to approximately 8 metres using Channel 1. If the receiver is 1 metre above the bottom we can expect these limits to increase to 11 and beyond 12 metres for Channels 4 and 1 respectively.

Figure 16 provides a similar plot for Target A in low power mode from Phase IV data. Note the increase in response variability in Channel 1. It indicates that the detection limit for Target A in low power mode based on Channel 4 would be 4 and 7 metres using receiver-bottom offsets of 2 and 1 metres respectively. Detection with Channel 1 is approximately 7 and beyond 12 metres, again for 2 and 1 metre offsets respectively.

An alternative approach for displaying the detection limits is to plot the signal strength at a set depth below the receiver against the receiver depth. Figure 17 is such a plot for the same Phase I data set used to produce Figure 15. Note that, based on a 2 metre Rx-Tx offset, the detection limits for

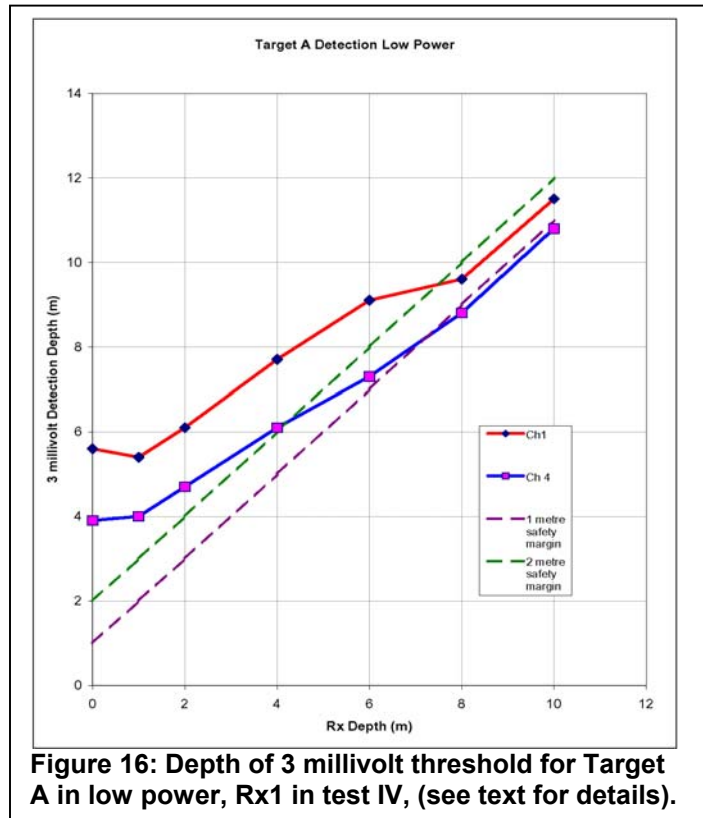


Figure 16: Depth of 3 millivolt threshold for Target A in low power, Rx1 in test IV, (see text for details).

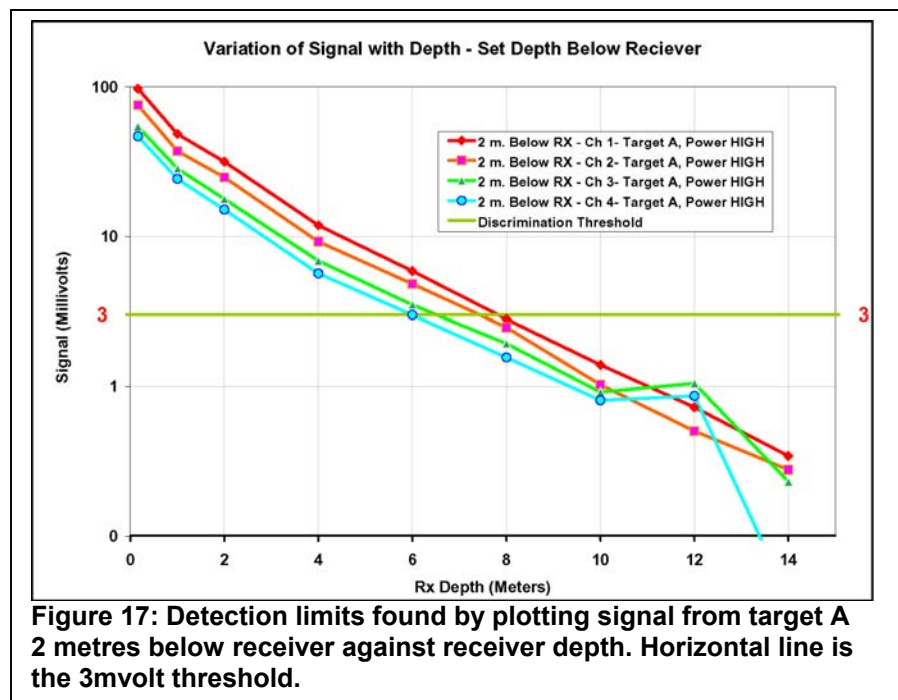


Figure 17: Detection limits found by plotting signal from target A 2 metres below receiver against receiver depth. Horizontal line is the 3mV threshold.

Channels 1 and 4 are respectively 8 and 6 metres as before. We do not have the flexibility with this presentation to assess how our detection varies with different receiver-to-bottom distances.

Figure 17 has a more explicit representation of the threshold than does Figure 15 and has the advantage that we can define depth limits using different threshold, for example 2 millivolts.

Figures 18 and 19 examine detection limits as a function of target size. Figure 18 is the type 2 detection plot for the 45 gallon (impl.) drum (our largest target) using a Rx/Tx offset of 2 metres. Figure 19 is a type 1 plot for our smallest target, Target I.

In Figure 18 the water depth at the test sites defined the lower limit for data collection. However, we can use the excellent data quality and linearity to predict the limit of detection to be slightly over 14 metres and 17 metres with Channels 4 and 1 respectively based on a 3millivolt threshold.

At the opposite size extreme, in Figure 19 we examine the depth of the 3 millivolt limit for Target I in high power mode. We can expect detection to depths of 4 and 6 metres for Channels 4 and 1 respectively if the receiver is 1 metre above the bottom, but these depths decrease to 1 metre for Channel 4 and 2 metres for Channel 1 if a 2 metre Rx/bottom offset is used.

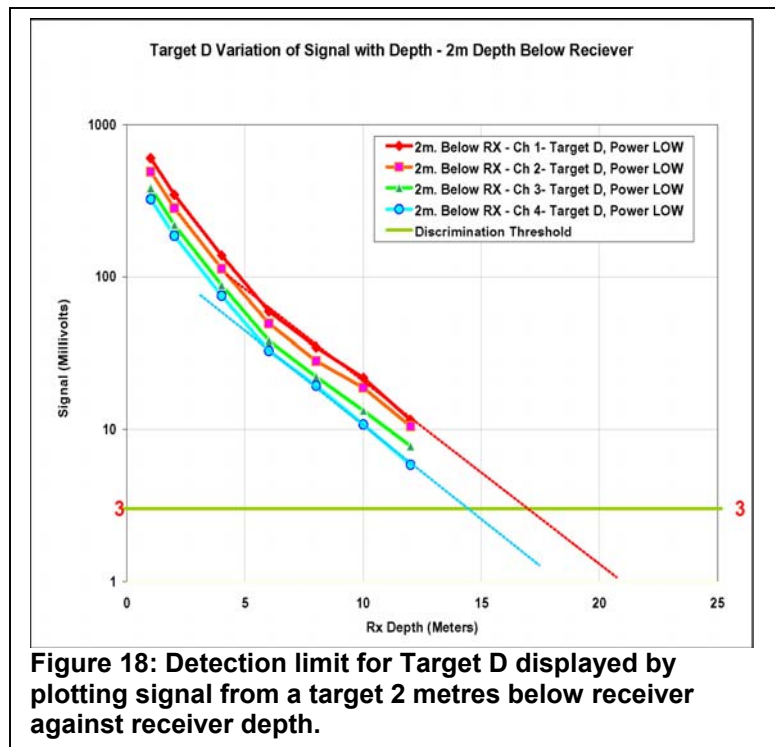


Figure 18: Detection limit for Target D displayed by plotting signal from a target 2 metres below receiver against receiver depth.

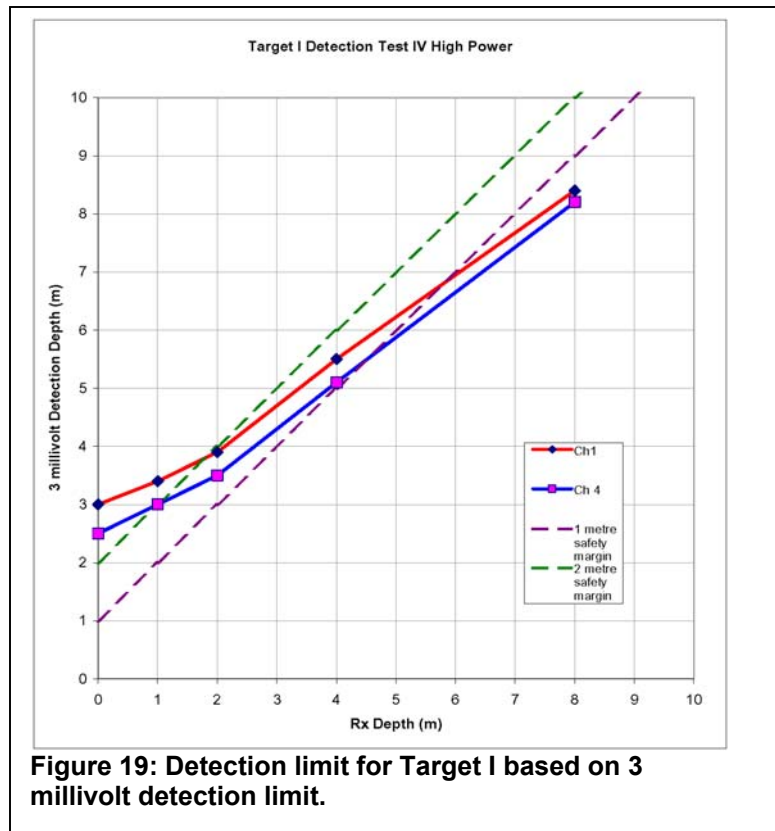


Figure 19: Detection limit for Target I based on 3 millivolt detection limit.

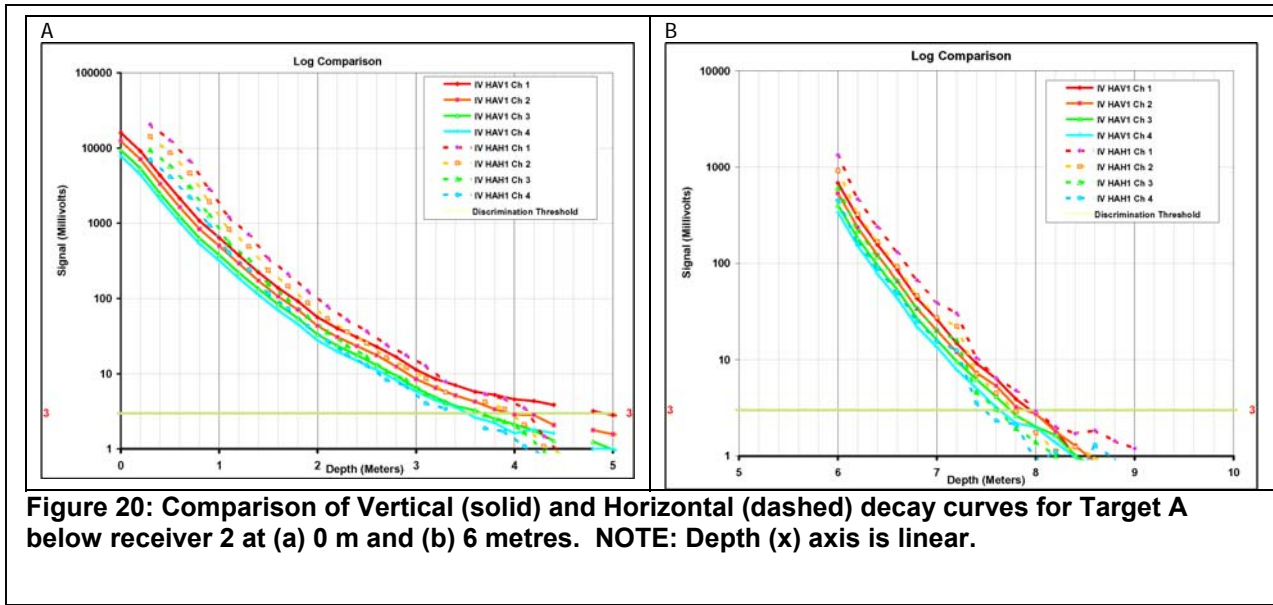


Figure 20: Comparison of Vertical (solid) and Horizontal (dashed) decay curves for Target A below receiver 2 at (a) 0 m and (b) 6 metres. NOTE: Depth (x) axis is linear.

3.10 Target orientation

The multiple parameters affecting the system response make it impractical to look at subtle changes in values associated with orientation of targets such as C that are almost symmetric, or small targets such as I. The largest change in response we can expect to occur from our most asymmetric target, “A”. Figure 20a and b compare the vertical (solid) and horizontal orientation (dashed) decays for Target A with the receiver Rx2 at 0 and 6 metres respectively. In these examples, the target is aligned with the long axis of the receiver when horizontal. For both Rx/Tx offsets, when the target is near the receiver coil the horizontal mode provides a stronger response, likely as a result of the proximity of the metal and the receiver coil. In both examples, one cannot differentiate the horizontal from vertical target response at the 3-millivolt limit of detection. Note that the horizontal data are more variable than the vertical, particularly in the deeper test. This is likely a result of difficulties in maintaining alignment of the target and the receiver.

3.11 Response Polarity

There were occasions during the survey at Wright’s Cove when the polarity of the response to targets would reverse without any change in the system set-up. The only configuration that created a negative response had the target outside the footprint of the receiver. Figure 21 shows data from Phase 1 (fresh water) where the receiver is set at 4 metres and the target is located 0.5 metres outside the long side of Rx1 coil.

Figure 22a shows the lateral response in Channel 4 in a cross-section from surface to 12 metres for Target A. Rx 2 is at 6 metres. Figure 22b is a similar cross-section for Rx2 at 2 metres and Target B (ball). Both Figures show the results for Channel 4. The other channels provide similar results with somewhat more extreme values.

Both figures show negative values outside the footprint and near the plane of the receiver. Target A (Figure 22a) creates a complex pattern in comparison to the simple ball of Target B (Figure 22b). The sharp lateral changes and shoulders are clearly visible on the sections and the response can vary drastically over very short distances. This implies the response to Target A is very unstable off to the sides. The instability appears to be largely a function of the elongated target based on the simple symmetry apparent in Figure 22b.

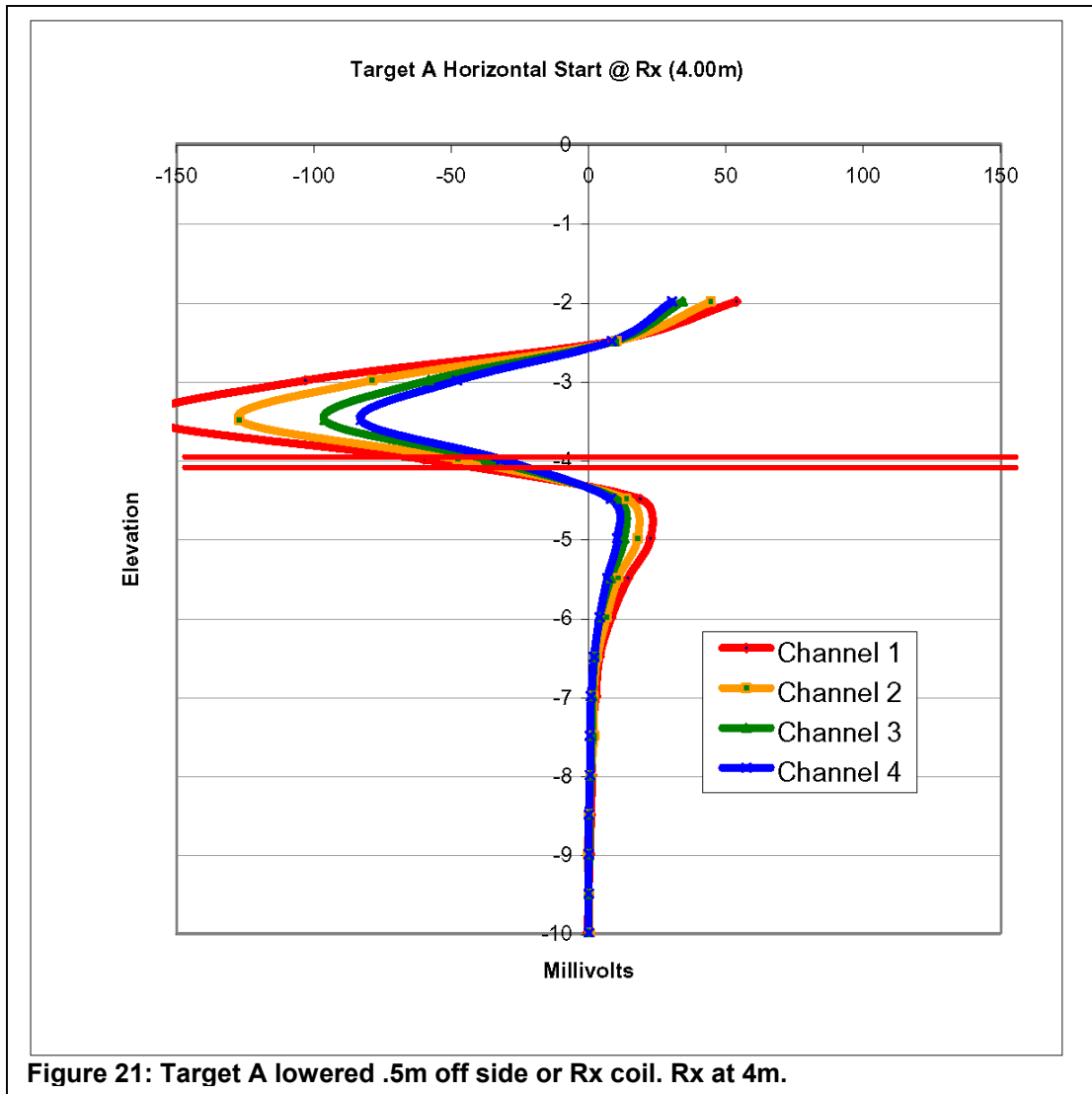


Figure 21: Target A lowered .5m off side of Rx coil. Rx at 4m.

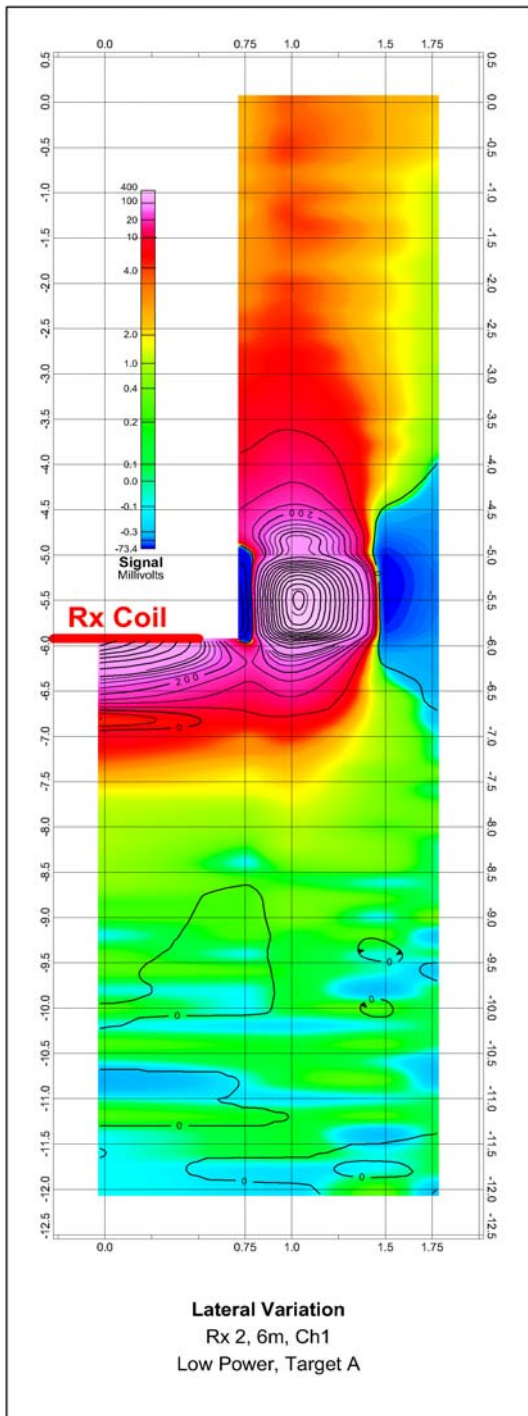


Figure 22a: Vertical cross-section (through long axis of the receiver) of response (millivolts) to Target A. RX2 at 6metres, axis in metres. Note orange & red positive, blue negative.

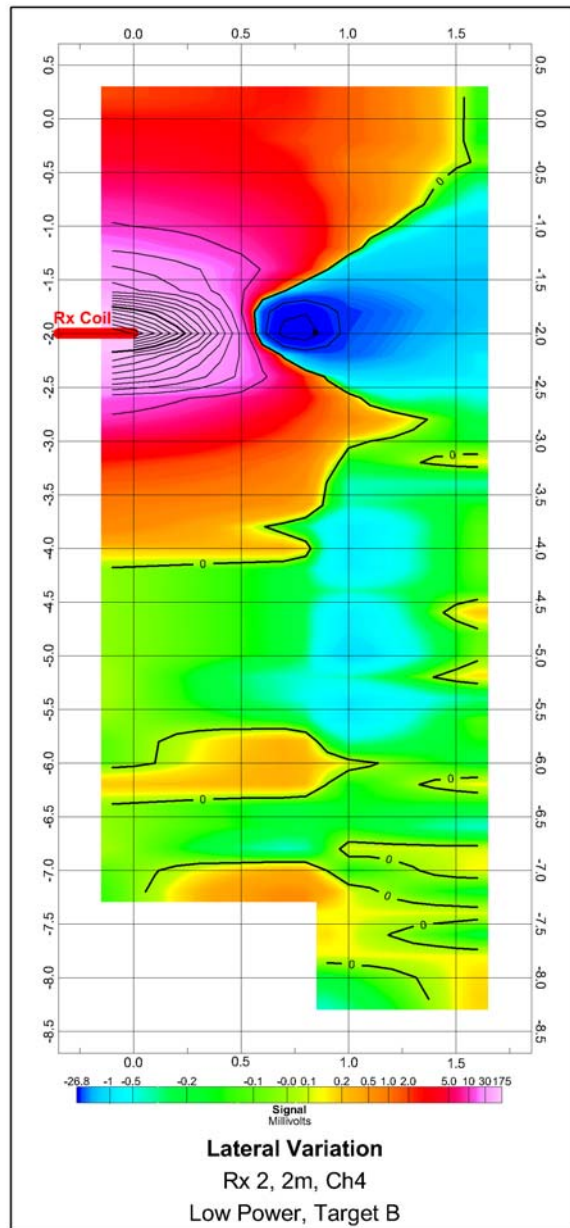


Figure 22b: Vertical cross-section (through long axis of the receiver) of response (millivolts) to Target B. RX2 at 2 metres, axis in metres. Note orange & red positive, blue negative.

4.0 CONCLUSIONS

The conclusions drawn from these tests are summarized in this section. These are addressed in the order that they were presented above, not necessarily in order of importance.

4.1 System Noise & Variability

4.1.1 Receiver Coils

As described in detail above, the receiver coil (Rx1) constructed by Geonics Limited for DCL has a hardware problem related to its electrical connection with the transmitter. The connector for the communications cable appears to be in contact with the windings. This problem could not be resolved within the time constraints of this project and a temporary solution was implemented. The signal from Rx1 (Tx in high power mode) is 2 to approximately 3 times (in low power) that of a standard underwater EM61 coil. Even with only a temporary methodology for reducing the electrical noise, Rx1 provided a better signal-to-noise ratio than the standard coil. The potential for superior performance by Rx1 was confirmed in the Phase I work where the ice provided electrical insulation between the transmitter and the receiver.

1. **The special receiver coil built for DCL is a significant improvement over the standard underwater coil.**

a. **High vs. Low Power**

The low power mode of the EM61MK2 provides a broader dynamic range of responses for the four data channels than does the high power at the same receiver and target depths. This broader range of values should provide better discrimination of targets, even though the high power mode provides a better signal-to-noise ratio. The change in the “dynamic range” of the channels is not a simple function of the power of the transmitted signal.

The response ratio in the gates for high and low power modes changes with the size of the target. Since the sampled windows (gates) of each channel are fixed relative to the peak current (start of the primary pulse), the “spread” must be related to the position of the gates in time with respect to the end of the pulse. This difference in the gate values does not reportedly occur in the standard version of the high power Em61Mk2 system and must therefore be a result of our unique use of a large loop transmitter. This would be consistent with the method the software uses to monitor and correction for decreasing signal. It is also notable that lengthening of the primary signal will change our frequency content; that will also affect the response, particularly for smaller targets.

Based on the fact that the system behaved as expected when comparing receiver coils Rx1 and Rx2 in high power mode we suspect the inconsistency occurs when the system is set in low power. That said, it would be highly desirable to have the spread in the channels provided by the low power mode with the improved signal-to-noise ratio of high power.

2. **There are inconsistencies in the fundamentals of the how the system is meant to and actually operates. These are most likely related to the data collection software. Until resolved, these issues preclude any attempt at modelling at this time.**
3. **The optimum configuration would be to have the time gate configuration of the low power mode with the signal-to-noise ratio provided of the high power system.**

4.2 Stationary Noise

The channel responses experience slow long-term drift that is of little concern in practise because it can be removed with simple high pass filtering (such as subtracting a moving average). The short-term variations displayed by the system are consistently low, ranging from 2 millivolts per sample for channel 1 and 1 millivolt per sample for channel 4. We have defined a “threshold” background noise of 3 millivolts, a conservative value recognizing the system is stationary in these tests and probably less noisy than when underway.

An unexpected result of the background tests was that in the absence of a target the system noise appeared to increase with depth (in a marine environment), particularly when using the high power mode. Later tests showed the response below the transmitter to be relatively insensitive to Rx offset and tilt; therefore we speculate that the increased noise was related to motion within the earth’s magnetic field.

4. **Noise levels decrease as we move from channel 1 to 4.**
5. **When stationary, typical channel 1 background noise is less than 3 millivolts. This is used as a threshold for detecting anomalies on all channels.**

4.3 Geometry

The receiver coil was rotated from the horizontal to determine the effect of tilt on the system response. The overall change in the response is consistent with the predicted cosinusoidal dependence on tilt angle; in more detail, however, the response is not as simple as expected.

6. **The limit of detection for a target does not noticeably change for small (<30 degree) misalignments of the receiver coil from its intended horizontal orientation.**
7. **The misalignment response itself can vary significantly and in a complex manner from that observed in the horizontal mode.**

Conclusion 7 has significant implications for prospects of developing target discrimination algorithms for this and other underwater EM systems (see section 4.11 below)

4.4 Response to lateral offsets of Rx and target from the axis of the transmitter.

Decay curves were collected using Target B in one quadrant below the transmitter with the receiver 2, 4 and 6 metres below the transmitter. The variations in response from set depths

below the receiver were plotted and contoured in the horizontal plane. The vertical position of the peak response changed from being in the plane of the receiver when the system was symmetrically centred beneath the transmitter to slightly above the Rx coil towards the edges of transmitter coil. The plotted results therefore varied depending on whether the values used were based on the depth below the receiver or relative to the peak value. As measured from the receiver the pattern was a rectangular plateau or “sweet-spot”, broader down the long dimension of the receiver. When the peak value was used as a reference, the sweet-spot was more square with the corners towards the centre of each of the transmitter sides. Since field measurements would be referenced to the receiver, our conclusions concerning lateral variations in response are as well.

- 8. The response to the target is relatively invariant over a three metre wide swath along the long dimension of the receiver at approximately 3 metres deep.**
- 9. The response along the short axis of the receiver decreases steadily from the centre, such that it is approximately of half the peak value when below (but inside) the transmitter loop.**

4.5 Tx Signal Strength

In section 4.3 we showed that increasing the transmitter loop size to 4 x 8 metres had minimal impact in spite of our increased power output. This is a result of the compromise between the increased signal strength and an increase in the distance of the Rx from the transmitter wire.

- 10. More energy can be achieved from a larger transmitter. For shallow work that benefit is negated by the distance from the transmitter loop.**
- 11. The details of the transmitter system and the associated compromises inherent in getting that energy require additional investigation.**

4.6 Salinity Variations

The background noise changes between tests conducted in waters of varying conductivity. However, the changes observed are relatively small and because of the problems with Rx1 and efforts to remedy that issue we cannot isolate variations due to Rx1 from the apparently minor changes in background noise that might result from water conductivity. We note that the small increase in noise levels between the fresh water and salt-water tests are not consistent with the several orders of magnitude difference in water conductivity and therefore do not appear to be related.

Tests with Target A exhibit essentially the same response in salt or fresh water regardless of the power mode of the system. However, the marine response-vs depth decay curves for Target F are consistently shifted downwards relative to their fresh water equivalent. The shift is between 0.15 and 0.35 metres. The rate of decay on a log-log scale is the same regardless of water salinity. It is possible that combined experimental error in measuring depth and, to a lesser degree, the buoyancy of saltwater (Tx- reference) account for part of the discrepancy. However the

appearance of the decay curve is not consistent with geometry accounting for the entire offset in values. Other factors could be variations in the frequency content of the signal at the target in the two media, and an increase in signal when the target time constant is similar to the pulse width.

- 12. The decay curves observed in salt and freshwater are very similar for Target A. Decay rates for the smaller Target F are the same but the overall depth variation is normally less than 0.15 metres, although one variation of 0.35 metres was observed.**
- 13. The marine responses for target F are a consistent percentage lower than the fresh water values. The discrepancy, if real, implies that maximum detection depth in a marine environment may be slightly less than in fresh water.**

4.7 Depth Limitations

We have collated the various decay curves for the different targets in two different types of plots that show detection depth. Detection will vary not only with the configuration of the system but also with both the signal-to-noise threshold chosen and the height of the receiver above the bottom. Type 1 plots require the detection threshold be specified and allows the interpreter to explore varying the receiver depth above the bottom. Type 2 plots fix the receiver-bottom distance and plot the signal against receiver depth. This provides superior signal quality and threshold sensitivity assessment.

We present depth limitation plots for our smallest (I-04 m² surface area -0.77kg) and largest (D-3.94 m² surface area-13.61kg a drum) targets. Detection depth improves in the earlier time gates with Channel 1 typically detecting targets 1-2 metres deeper than Channel 4.

- 14. The maximum depth of detection for an object the size of a 45 imperial gallon drum, assuming a 2-meter receiver-bottom offset and a 3millivolt threshold, is 17 metres (Channel 1).**
- 15. The maximum depth of detection for an object the size of a small projectile (cross-section 0.04 m²) assuming a 2-meter receiver-bottom offset and a 3millivolt threshold is 4 metres (Channel 1).**

4.8 Response Polarity

Various configurations of the system geometry were assessed in an attempt to duplicate a reversal in target polarity that was observed in a previous survey. Only one configuration was identified that would create the desired reversal; that was a metal object that passed beside and outside the footprint of the receiver coil. The response was repeated with several targets. The response was shown to be stable for a symmetric target such as a ball but highly unstable for an asymmetrical target such as a pipe.

- 16. The most like cause of polarity reversals in previous surveys was a target located beside the footprint of the receiver (geometrical factor/coupling).**

4.9 Modeling

We were unsuccessful in attempts to adapt the EMIGMA forward modeling program developed by Petros Eikon Limited to duplicate the early field data and abandoned additional efforts because modeling was not the primary focus of this project. It is our understanding that more robust algorithms, that scale down to the size of our targets, have and are being developed. We cannot comment on those. We have noted several inconsistencies (conclusion 2 above) between our observations and how the system was expected to behave that must be resolved prior to a concerted modeling effort, or the modeling results could not be effectively calibrated. There are several layers of variability in the results that may preclude an effective discrimination algorithm (see conclusion 2).

- 17. Modeling the results from this system require resolution of a number issues with the Geonics high-powered EM61-MK2 system.**
- 18. The level of spatial variability inherent in the system makes the prospect of a reliable algorithm for discrimination poor.**

5.0 RECOMMENDATIONS

The next logical step in determining the capabilities of this system are related to both the transmitter loop size and limitations imposed by motion. Below we provide recommendations with regard to the focus of future work and specific lessons learned from this effort.

The cause of the difference in the “spread” between channels in low and high power needs to be identified.

A permanent solution for the electrical noise must be implemented.

The potential for variation in the transmitter loop and size requires testing and sensitivity analysis.

The system needs to be tested under motion and in the presence of waves, noise levels established and methodologies for identifying the location of the receiver below the transmitter designed and tested.

Logistically it is simpler and more cost effective to conduct the majority of the testing in fresh water, but some further testing in a marine environment is warranted to confirm the conclusion that the water conductivity has little influence, particularly at the noise limits of the system.

The system was intended to provide a cost effective platform for detection of accumulations of underwater UXO to depths in excess of ten metres while minimizing seabed contact. Although currently the system deploys a single receiver, expansion to multiple receivers appears to be possible. The key advantages of this system are:

Cost: the system can be deployed for under \$100K;

- Flexibility: the system does not require a specific dedicated boat and can be deployed from any vessel of appropriate size and draft;
- Simplicity: The system is composed of existing and readily available components. Repairs are relatively simple and redundant components can be affordably deployed therefore minimizing down time;

Adaptability: Although the current system is deployed using Geonics’ components, the approach can be adapted to most manufacturers’ sensor systems.

Overall the system has performed well. Although some issues with electrical noise existed, the source of this noise has been identified and can be removed. When electrically isolated the system has a noise level better than the 3 millivolts used here. The system has a demonstrated potential for detecting underwater UXO (depending on size) in water depths of over 10 metres without contacting the bottom.

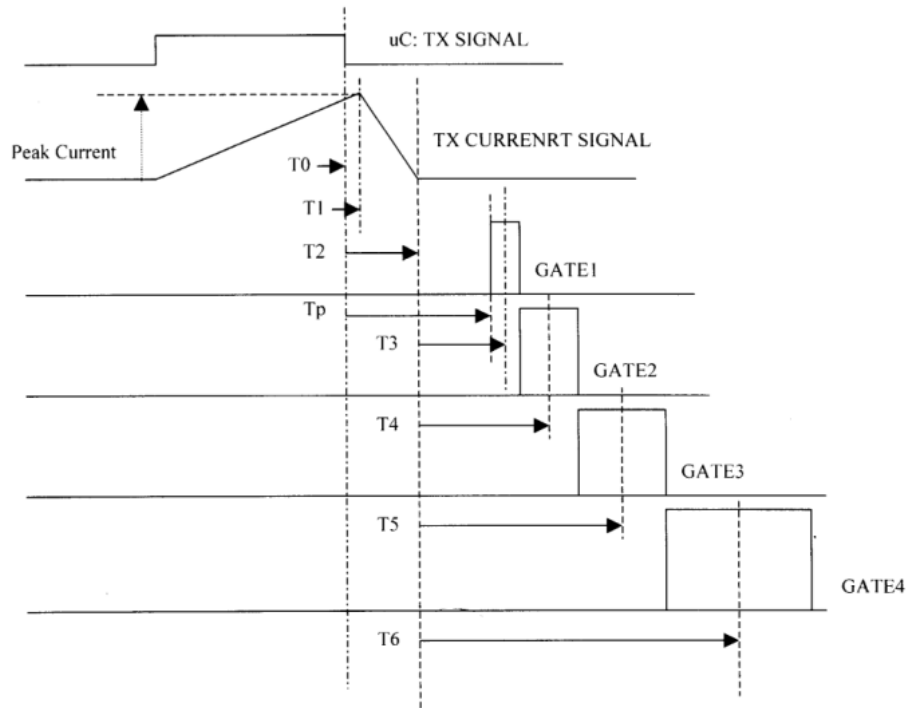
The prototype system has accomplished its goals in stationary mode but these tests have also highlighted a number of potential questions regarding the application of this and other EM systems underwater.

APPENDICES

A1 – Geonics’ Time gate Figure

FEB 5, 2003

EM61MK2HP TIMING



	T1(uS)	T2(uS)	T3(uS)	T4(uS)	T5(uS)	T6(uS)	Peak Current*(A)
HIGHPWL	20	76	317	432	583	782	6.02
HIGHPWH	20	132	261	376	527	726	12.04

*Peak Current measure at 12.39V Battery input. Unit is (A).

Start position & Gate Width

	Tp(uS)	Gate1 Width(uS)	Gate2 Width(uS)	Gate3 Width(uS)	Gate4 Width(uS)	TOP GATE(uS)
HIGHPWL	345	100	131	172	226	172
HIGHPWH	345	100	131	172	226	172

DETAILS OF TIME GATES PROVIDED BY GEONICS LIMITED

A2 – Details of Targets

Target	A	B	C	D	E	F	G	H	I	L
										
Length	0.89		0.32	0.96	0.41		0.33	0.41	0.17	1.07
Diameter	0.1	0.22	0.17	0.6	0.05		0.075	0.04	0.05	0.27
Weight (kg)	14.06	11.62	44.45	13.61	2.2	8.16	2.29		0.77	0.33
Surface Area (m ²)	0.54	0.15	0.46	3.94		0.08	0.12	0.07	0.04	0.89
Metal Vol. (m ³)	0.001492	0.005575	0.005801	0.000857		0.001345	0.000348	0.000834	0.000098	

A3 – Specific Tests

PHASE II

Date	Tests	TX		RX			Target					Power	File			Line	Tran	Comments	Conditions			
		X	Y	X	Y	Z	Type	Orien	X	Y	Z Start		Z End	Z Inc	Raw					Tr	XLS	
19/07/05	Cond					Start	End	inc	None													
	Back 1 LP	0	0	0	0	0	0							Low	lpBack1	X	Backgrounds II	0	042216	Conductivity Test	Wet damp	
						1	1								LPBack2	X	Backgrounds II	1.01	042216			
						2	2								LPBack3A	X	Backgrounds II	2	042216	renulled		
						4	4								Back4	X	Backgrounds II	4	042216			
						6	6								LPBack5	X	Backgrounds II	6	042216			
						8	8								Back6	X	Backgrounds II	8	042216			
						8	8								LPBack7	X	Backgrounds II	8	042216	Moved boat off Barge		
						8	8								LPBack8	X	Backgrounds II	8	042216	Switched recorder setting to HP (but not battery, it is still in		
						6	6								LPBack9	X	Backgrounds II	6	042216			
						4	4								LPBack10	X	Backgrounds II	4	042216			
						2	2								LPBack11	X	Backgrounds II	2	042216			
						1	1								LPBack12	X	Backgrounds II	1	042216			
						0	0								LPBack13	X	Backgrounds II	0	042216			
					0	0							High	HPBack1	X	Backgrounds II		042216				
					1	1								HPBack2	X	Backgrounds II		042216				
					2	2								HPBack3	X	Backgrounds II		042216				
					4	4								HPBack4	X	Backgrounds II		042216				
					6	6								HPBack5	X	Backgrounds II		042216				
					8	8								HPBack6	X	Backgrounds II		042216	Renulled @ 140m			
					10	10								HPBack7	X	Backgrounds II		042216	system surging			
					10	10								HPBack8	X	Backgrounds II		042216	TX battery replaced			
					12	12								HPBack9	X	Backgrounds II		042216				
					12	12							Low	LP14	X	Backgrounds II		042216	Logger battery died			
20/07/05	Back					2	2						Low	LPBack B1	X	Backgrounds II		042223		Foggy & Muggy		
						2	2						High	HP Back B1	X	Backgrounds II		042223				
	Ord Decay					0	12	1.2	A	V	0	0	0	0.2	High	havc	X	Decays II		042223		
						0	12	1.2	A	V	0	0	0	0.2	Low	LAVC	X	Decays II		042223		
						0	8	1.2	E	V	0	0	0	0.2	Low	LEVC	X	Decays II		042223		Hot & Sunny
						4	12	2	E	V	0	0	0	0.2	Low	LEVC2	X	Decays II		042223	Switched Batteries, REPEAT DATA	
						0	1	1	E	V	0	0	0	0.2	High	PEVC	X	Decays II		042223	Tran quit	
						0	8	1.2	B		0	0	0	0.2	Low	LBC	X	Decays II		042216	New Tran	
	Back/Ord					2	2		B		0	0	0	0.2	Low	LBC	X	Decays II		042216	Pulled ball through coil at end of test	
	Off Test	0	0	0	0	1	4	1.2	B		0	1.15	1, 2, 4	0.2	Low	LB off A	X	Vry Geom		042216	Target starts at water surface	
	Off Test					1	4	1.2	B		-1.5	1.15	-1,-2,-4	0.2	Low	LB off B	X	Vry Geom		042216	Target starts at water surface	
	Rx Alignment					2	2	0	B		0	0	-2	0.2	Low	LB Ang Rx	X	Vry RX Ang		042216	Target starts at water surface	
	Rx Alignment					2	2	0	A	V	0	0	-2	0.2	Low	LA Ang Rx	X	Vry RX Ang		042216	Target starts at water surface	
	Off Test	0	0	0	0	1	4	1.2	A	V	0	1.15	-1,-2,-4	0.2	Low	LA off A	X	Vry Geom		042216	Target starts at water surface	
Off Test					1	4	1.2	A	V	-1.5	1.15	-1,-2,-4	0.2	Low	LA off B	X	Vry Geom		042216	Target starts at water surface		
Ord Decay					0	12	1.2	A	H	0	0	0	0.2	Low	LAHC	X	Decays II		042216	Target Aligned with Rx		
Ord Decay					0	12	1.2	A	H	0	0	0	0.2	Low	LAHOC	X	Decays II		042223	Target across Rx	Hot & Sunny	
Metal Decay					0	10	1.2	D	V	0	0	0		Low	LDVC	X	Decays II		042223			
					0	6	1.2	D	V	0	0	0		High	HDVC	X	Decays II		042223	System in Oscillation		
					4	8	2	D	V	0	0	0		High	HDVC-B	X	Decays II		042223	New Batteries		
					0	10	1.2	D	H	0	0	0		Low	LDH1C	X	Decays II		042223	Target Aligned with Rx		
Ord Decay					0	10	1.2	F	H	0	0	0		Low	LFHC	X	Decays II		042223	Target Aligned with Rx		
					0	0	1.2	F	H	0	0	0		High	HFHC	X	Decays II		042223	Target Aligned with Rx, NO Responce		
					0	6	1.2	F	H	0	0	0		High	HFHC-2	X	Decays II		042216	Target Aligned with Rx, L4 noisy		
					0	12	1.2	F	V	0	0	0		Low	LFVC	X	Decays II		042216			
					0	10	1.2	G	V	0	0	0		Low	LGVC	X	Decays II		042216	Spike on L2		
					0	10	1.2	H	H	0	0	0		Low	LHHC	X	Decays II		042216	Target Aligned with Rx		
					0	10	1.2	H	V	0	0	0		Low	LHVC	X	Decays II		042216			
					0	8	1.2	I	H	0	0	0		Low	LIHC	X	Decays II		042216	Target Aligned with Rx		
22/07/05						0	0	1.2	C	H	0	0	0			LCHC	X	Decays II		042223	Target Aligned with Rx, Prob w Tran	Hot & Sunny
						0	6	1.2	C	H	0	0	0			LCHC-2	X	Decays II		042216	Target Aligned with Rx, Tx prob	
						6	12	2	C	H	0	0	0			LCHC-3	X	Decays II		042216	Target Aligned with Rx, New Bat	
	Off Test					2	6	2	B		0.5	0	-2,-4,-6			B off 5				042216	Rotated RX 90deg Target off side (shrt edge) Target starts	
						2	6	2	B		1	0	-2,-4,-6							042216	Target starts at water surface	
						2	2	0	B		1.5	0	-2							042216	Target starts at water surface, Tran Prob	
	Off Rx			0	0	2	6	2	B		0	0	-2,-4,-6			B off Rx				042223		
				0	1	2	6	2	B		1	0	-2,-4,-6			B off Rx1				042223		
				0	2	2	6	2	B		1	0	-2,-4,-6			B off Rx2				042223	New Battery	
	Metal Decay					0	6	1.2	L	H	0	0	0		Low	LCH	X	Decays II		042223	Target Aligned with Rx, Noisy Unstable	
						6	6		L	H	0	0	0		Low	LCH-2	X	Decays II		042216	Target Aligned with Rx, flat response	
						6	10	1.2	L	H	0	0	0		Low	LCH-3	X	Decays II		042223	Target Aligned with Rx, 2 bats in parrallel	
	Off Rx	1	0	0	1	2	6	2	B		0	0	-2,-4,-6			B off Rx3				042223	Moved 1X 1m	
						1	0	0	2	2	6	2	B							042223	Moved TX 1m	
					2	0	0	2	2	6	2	B							042223	Moved TX 2m		

Phase III

Date	Tests	TX		RX			Target					File			Line	Tran	Comments	Conditions					
		X	Y	X	Y	Z			Type	Orien	X	Y	Z Start	Z End					Z Inc	Power	Raw	Tr	XLS
						Start	End	inc															
5/10/2005	Back LP	0	0	0	0	0	16	1,2	None								Low	LB0					See notes regarding boat movement & instrument drift,
	Back HP					16	-2	2,1									High	HB1					L-2 is a test of having Eli drape legs in and out of water (sh
	Back HP					0	2	2										HP2					Draped part of coil into water 1st one sied and then both
	Back LP					2	2											LB1					Tests of having sides of coil in water on LP / Checked to see
	Back LP					2	2											LB3					Lowered Tx all into water -Logger died
	Back HP					2	10	8										HP3					tested HP effects w Tx in water Noted issues related to vari

Phase IV

Date	Tests	TX		RX						Target						File			Line	Tran	Comments	Conditions		
		X	Y	Coil	X	Y	Z			Type	Orien	X	Y	Z Start	Z End	Z Inc	Power	Raw					Tr	XLS
							Start	End	inc															
26/10/2005	Back LP	0	0	2	0	0	0	15	1,3,5	None							Low	LPB1	x	Backgrounds IV				Sunny cool
	Back HP			2	0	0	15	10	5								High	HPB1	x	Backgrounds IV				
	Ord Decay			2	0	0	0	14	1,2	A	V	0	0	0	varies	0.2	Low	LA1	x	Decays IV				
				2	0	0	0	14	1,2	A	V	0	0	0	varies	0.2	High	HAV1	x	Decays IV				
				2	0	0	0	10	1,2	A	H	0	0	0	varies	0.2	High	HAH1	x	Decays IV				10m tests have horiz positioning issues due to wind
				2	0	0	0	10	1,2	B		0	0	0	varies	0.2	High	HBALL	x	Decays IV				
				2	0	0	10	0	-2,-1	B		0	0	0	varies	0.2	High	LBALL	x	Decays IV				
				2	0	0	0	14	1,2	F	V	0	0	0	varies	0.2	Low	LFV1	x	Decays IV				
27/10/2006	Ord Decay			2	0	0	0	10	1,2	I	V	0	0	0	varies	0.2	Low	LIR2	x	Decays IV				
				2	0	0	0	12	1,2	I	V	0	0	0	varies	0.2	High	HIR2	x	Decays IV				
				2	0	0	0	12	1,2	F	V	0	0	0	varies	0.2	High	HFVR2	x	Decays IV				
	Rx Alignment			2	0	0	2	2	0	B		0	0	-2		0.2	High	HR2AL	x	Others IV				Receiver Alignment Offset 0.05-0.2m
	Rx Alignment			2	0	0	2	2	0	B		0	0	-2		0.2	Low	LR2AL	x	Others IV				Receiver Alignment Offset 0.05-0.2m
	Off Test	0	0	2	0	0	2	6	4	B		0	0.75	-2		0.2	Low	BoffR2	x	Others IV				Target off side in RX, Rotated Rx 90 deg
	Off Test	0	0	2	0	0	2	6	4	A		0	0.75	-2		0.2	Low	AoffR2	x	Others IV				Target off side in RX, Rotated Rx 90 deg
	Rx Alignment			2	0	0	2	2	0	A	V	0	0	-2		0.2	Low	LAR2al	x	Others IV				Receiver Alignment Offset 0.05-0.2m
	Rx Alignment			2	0	0	2	2	0	A	V	0	0	-2		0.2	High	LAR2al	x	Others IV				Receiver Alignment Offset 0.05-0.2m
	Tx Flip			2	0	0	2	2	0	A	V	0	0	-2		0.2	Low	LAR2FLT	x	Others IV				Checked polarity effects of Tx orientation by flipping connect
	Ord Decay			1	0	0	0	12	1,2,4	A	V	0	0	0	varies	0.2	Low	LAVR1	x	Decays IV				
				1	0	0	0	12	1,2,4	A	V	0	0	0	varies	0.2	High	HAVR1	x	Decays IV				
				1	0	0	0	12	1,2,4	F	V	0	0	0	varies	0.2	High	HFVR1	x	Decays IV				
				1	0	0	0	12	1,2,4	F	V	0	0	0	varies	0.2	Low	LFVR1	x	Decays IV				
				1	0	0	0	12	1,2,4	I	V	0	0	0	varies	0.2	Low	LIVR1	x	Decays IV				
				1	0	0	0	12	1,2,4	I	V	0	0	0	varies	0.2	High	HIVR1	x	Decays IV				
				1	0	0	0	12	1,2,4	B		0	0	0	varies	0.2	High	HBR1	x	Decays IV				
				1	0	0	0	12	1,2,4	B		0	0	0	varies	0.2	Low	LBR1	x	Decays IV				
27/10/2007	Trg Back LP			1	0	0	2	4	2	B		0	0	1	1		Low	LBRR1	x	Backgrounds IV				
	Trg Back HP			1	0	0	2	4	2	B		0	0	1	1		High	HBBR1	x	Backgrounds IV				
	Off Rx			1	0	1,2	2	6	2	B		0	0	-2,-4,-6			Low	OffR1B1	x	Others IV				Stepped Rx from Center to edge of Tx Tar centered in Rx
	Off Rx	1,2	0	1	0	0,1,2	2	6	2	B		0	0	-2,-4,-6			Low	OffR1B2	x	Others IV				Tx back 1m & 1.8, Stepped Rx from Center to edge of Tx T
	Trg Back LP			2	0	0	2	4	2	B		0	0	1	1		Low	LBRR2	x	Backgrounds IV				
	Trg Back HP			2	0	0	2	4	2	B		0	0	1	1		High	HBBR2	x	Backgrounds IV				
	Lrg Tx			2	0	0	2	14	4	B		0	0	0	varies		Low	LT2R2B	x	Others IV				Used Larger Tx cable but loop same size
	Lrg Tx			2	0	0	2	14	4	B		0	0	0	varies		Low	LT3R2B	x	Others IV				Increase Loop size to 4.3 X 8m
	Cond																							Conductivity Test
NOTES	R1 Taped connector well with plumber's tape																							

A4 Field Data (Digital)

The field data for the various tests detailed in Appendix A3 are provided digitally on the accompanying CD.

A5 Summary of Tests

Test	Target Orientation	Power Level	Rx – Tx Configuration	Comments
Video				Examine Lake Bottom
EM39				Measure vertical variation of water column conductivity
Back 1		LP		Variation in receiver response at shallow water depth (triggered manually)
Target A	Vertical	LP	Centralized	Vertical decay in instrument response at Rx depths ranging from 0.093 to 14 metres
Move Tx		LP	Varying	Measure background Rx response at depths from 1 to 14m at various locations within Tx coil
Back 2		LP	Centralized	Rx at 5m measured Rx variability at highest time interval (10/sec)
Back 2		HP	Centralized	Rx at 5m measured Rx variability at highest time interval (10/sec)
Target A	Vertical	HP	Centralized	Vertical decay in instrument response at Rx depths ranging from 1 to 14 metres
Target D	Horizontal	LP	Centralized	Vertical decay in instrument response at Rx depths ranging from 1 to 12 metres
Target A	Horizontal	LP	Centralized	Vertical decay in instrument response at Rx depths ranging from 1 to 12 metres
Target A various locations	Vertical	LP	Coils centralized, target varies	Vertical variation in instrument response with Rx at 4m and target ranging from 2 to 14 metres
Target E 40mm	Vertical	LP	Centralized	Vertical decay in instrument response at Rx depths ranging from 1 to 14 metres
Target C 86lb	Vertical	LP	Centralized	Vertical decay in instrument response at Rx depths ranging from 1.0 to 14 metres
Target A various locations	Vertical	LP	Tx shifted, target varies	Vertical variation in instrument response with Rx at 4m and target ranging from 2 to 14 metres